

ESD ACCESSION LIST

TRI Call No. 74895

Copy No. 1 of 1 cys.

TRI FILE COPY

ESD RECORD COPY
RETURN TO
SCIENTIFIC & TECHNICAL INFORMATION DIVISION
(TRI), Building 1210

Technical Note

1971-40

R. L. Bagley

The Analysis
of Two Simple Composite Structures
Using Mechanical Admittance Methods

7 September 1971

Prepared under Electronic Systems Division Contract F19628-70-C-0230 by

Lincoln Laboratory

MASSACHUSETTS INSTITUTE OF TECHNOLOGY

Lexington, Massachusetts



A00732219

Approved for public release; distribution unlimited.

MASSACHUSETTS INSTITUTE OF TECHNOLOGY
LINCOLN LABORATORY

THE ANALYSIS
OF TWO SIMPLE COMPOSITE STRUCTURES
USING MECHANICAL ADMITTANCE METHODS

R. L. BAGLEY

Group 73

TECHNICAL NOTE 1971-40

7 SEPTEMBER 1971

Approved for public release; distribution unlimited.

LEXINGTON

MASSACHUSETTS

The work reported in this document was performed at Lincoln Laboratory, a center for research operated by Massachusetts Institute of Technology, with the support of the Department of the Air Force under Contract F19628-70-C-0230.

This report may be reproduced to satisfy needs of U.S. Government agencies.

THE ANALYSIS OF TWO SIMPLE
COMPOSITE STRUCTURES USING
MECHANICAL ADMITTANCE METHODS

RONALD LAIRD BAGLEY

Submitted to the Department of Aeronautics
and Astronautics on September 1, 1971
in partial fulfillment of the requirements
for the degree of Master of Science

ABSTRACT

Mechanical admittance methods are applied to two simple composite structures. The mechanical admittances of the composite structures are predicted using the mechanical admittances measured on their constituent substructures. The effects of the suspension system on the measured admittances are estimated. Attention is devoted to the technique of analytically assembling substructures into a composite structure.

Resonant frequencies and mode shapes of the composite structures are estimated from the predicted admittances. The effects of modal participation and damping on the estimated mode shapes and resonant frequencies are discussed.

Thesis Supervisor: Louis L. Bucciarelli, Jr.
Title: Assistant Professor of Aeronautics and Astronautics

Accepted for the Air Force
Joseph R. Waterman, Lt. Col., USAF
Chief, Lincoln Laboratory Project Office

ACKNOWLEDGMENTS

I would like to take this opportunity to thank Professor Louis Bucciarelli Jr., my thesis advisor, for his guidance and patience in the completion of this thesis. I am also grateful for his interest in my ideas and his encouragement during the past five years.

Too much appreciation can not be expressed to the MIT Lincoln Laboratory, which provided me with the equipment, financial support and the people who have supported me in this project. In particular, I would like to thank Eric Stevens for his instruction and help in the operation of the IBM 360 time-sharing system. Also I am indebted to John Connelly and William Sheehan of Group 76 for their invaluable technical assistance. Credit is due to Sara McNeil of the library staff for her extensive search for publications relevant to the topic of this thesis. Finally, I would like to thank the following members of Group 71 for their help with a myriad of problems and important details: Howard Faulkner, Marvin Pope, Roy Purdy and Ed Sweeney.

The photographs for this thesis are the work of the Audio-Visual Section of Lincoln Laboratory.

TABLE OF CONTENTS

| CHAPTER | | PAGE |
|---------|--|------|
| I | Introduction | 12 |
| II | Analytical Basis | |
| | 2.1 The Mechanical Admittance and Mechanical Impedance of a Structure | 14 |
| | 2.2 Assembling Substructures into a Composite Structure Using Mechanical Impedance Notation | 21 |
| | 2.3 The Effect of Damping on Resonant Frequencies and Admittances | 26 |
| | 2.4 Estimating Resonant Frequencies and Mode Shapes for Composite Structures from Predicted Admittance Data | 30 |
| III | The Mechanical Admittance Measurement and Prediction System | 38 |
| IV | Experimental Results | |
| | 4.1 Introduction to Experimental Results | 47 |
| | 4.2 The Effects of the Suspension System, Impedance Head and Shaker on the Measured Admittances of a 40-Inch Free Rod | 49 |
| | 4.3 Predicting the Admittances, Resonant Frequencies and Mode Shapes for an 80-Inch Free Rod | 61 |
| | 4.4 The Effects of the Suspension System on the Measured Admittances of a 32-Inch Free Beam | 73 |
| | 4.5 Predicting the Admittances, Resonant Frequencies and Mode Shapes for a 42-Inch Composite Beam | 88 |

| CHAPTER | | PAGE |
|------------|--|------|
| IV | Experimental Results (cont.) | |
| | 4.6 Conclusions | 100 |
| APPENDICES | | |
| A | The Triangular Decomposition Method of Matrix Inversion | 101 |
| B | Computer Program Listings | 103 |
| REFERENCES | | 114 |

LIST OF FIGURES

| Number | Title | Page |
|--------|---|------|
| 2.1 | Schematic of the Degrees of Freedom of the Finite Element Idealization of a Continuous Structure | 14 |
| 2.2 | Schematic of Substructures To Be Assembled into a Composite Structure | 21 |
| 2.3 | Schematic of Assembled Composite Structure | 23 |
| 2.4 | Plots of Equation 2.54 for Different Values of the Parameters d_n , α , and β | 33 |
| 2.5 | The Modal Participation Vectors of the p^{th} and j^{th} Modes in the Complex Plane | 34 |
| 3.1 | The Mechanical Admittance Measurement and Prediction System | 39 |
| 3.2 | Schematic of Shaker and Impedance Head | 40 |
| 3.3 | Schematic of the SD1002B-33 Automatic Mechanical Impedance System in the Mechanical Admittance Mode | 41 |
| 3.4 | Schematic of the Transfer Function of a SD101A Filter in the Frequency Domain | 42 |
| 3.5 | The SD1002B-33 Automatic Mechanical Impedance System and Charge Amplifiers | 44 |
| 4.1 | Schematic of Assembling Two Composite Structures from Their Constituent Substructures | 47 |
| 4.2 | Measuring the Cross-admittance of a 40-inch Steel Rod | 48 |
| 4.3 | The Lumped Parameter Model of the Rubber Band and Rod Ensemble | 49 |
| 4.4 | Lumped Parameter Model of a Free Rod | 51 |
| 4.5 | Schematic of a Free Rod | 54 |
| 4.6 | Admittance (11) Measured for 40 Inch Rod | 55 |

| Number | Title | Page |
|--------|--|------|
| 4.7 | Admittance (11) Calculated for 40 Inch Rod | 56 |
| 4.8 | Admittance (21) Measured for 40 Inch Rod | 57 |
| 4.9 | Admittance (21) Calculated for 40 Inch Rod | 58 |
| 4.10 | Schematic of Measuring the Admittances for a 40-Inch Rod | 61 |
| 4.11 | Schematic of Assembling an 80-Inch Rod from Two 40-Inch Rods | 62 |
| 4.12 | Admittance (11) Predicted for 80 Inch Rod | 63 |
| 4.13 | Admittance (21) Predicted for 80 Inch Rod | 64 |
| 4.14 | Admittance (31) Predicted for 80 Inch Rod | 65 |
| 4.15 | Admittance (22) Predicted fro 80 Inch Rod | 66 |
| 4.16 | Admittance (11) Calculated for 80 Inch Rod | 67 |
| 4.17 | Admittance (21) Calculated for 80 Inch Rod | 68 |
| 4.18 | Admittance (31) Calculated for 80 Inch Rod | 69 |
| 4.19 | Admittance (22) Calculated for 80 Inch Rod | 70 |
| 4.20 | Suspension System Used to Measure the Admittances of a 32-Inch Free Beam | 74 |
| 4.21 | Measuring a Mutual Admittance of a 32-Inch Free Beam | 75 |
| 4.22 | Measuring a Cross Admittance of a 32-Inch Free Beam | 76 |
| 4.23 | Admittance (22) for a 32-Inch Beam | 77 |
| 4.24 | Admittance (22) for a 32-Inch Beam | 78 |
| 4.25 | Schematic of 32-Inch Beam Suspension System | 79 |
| 4.26 | Schematic of the Reaction Forces in the Suspension System | 80 |
| 4.27 | Admittance (11) Measured for 32 Inch Beam | 83 |
| 4.28 | Admittance (21) Measured for 32 Inch Beam | 84 |

| Number | Title | Page |
|--------|--|------|
| 4.29 | Admittance (31) Measured for 32 Inch Beam | 85 |
| 4.30 | Admittance (22) Measured for 32 Inch Beam | 86 |
| 4.31 | Admittance (32) Measured for 32 Inch Beam | 87 |
| 4.32 | Half Scale Cross Section of the Channel | 88 |
| 4.33 | The Locations of the Measured Admittances for a 32-inch Beam | 89 |
| 4.34 | Assembling a 42-inch Composite Beam from Two 32-inch Free Beams | 90 |
| 4.35 | Admittance (11) Predicted for 42 Inch Beam | 91 |
| 4.36 | Admittance (21) Predicted for 42 Inch Beam | 92 |
| 4.37 | Admittance (31) Predicted for 42 Inch Beam | 93 |
| 4.38 | Admittance (41) Predicted for 42 Inch Beam | 94 |
| 4.39 | Admittance (22) Predicted for 42 Inch Beam | 95 |
| 4.40 | Admittance (32) Predicted for 42 Inch Beam | 96 |

LIST OF TABLES

| Number | Title | Page |
|--------|--|------|
| 4.1 | Properties of a 40-inch Steel Rod | 59 |
| 4.2 | Calculated and Predicted Mode Shapes and Resonant Frequencies | 71 |
| 4.3 | Comparison of Measured and Calculated Resonant Frequencies for a 32-inch Free Beam | 82 |
| 4.4 | Physical Properties of a 32-inch Beam | 88 |
| 4.5 | Calculated and Predicted Mode Shapes and Resonant Frequencies for a 42-inch Composite Beam | 98 |

LIST OF SYMBOLS

- $[C]$: a flexibility matrix
 $[C^*]$: a diagonal damping matrix
 $[J]$: the participation of the j^{th} mode in the admittance matrix
 $[K]$: a stiffness matrix
 $[M]$: a mass matrix
 $\{Q\}$: a column matrix of generalized forces
 R : deadweight reaction forces
 $\{u\}$: a column matrix of generalized displacements
 W : a deadweight load
 Y : admittance
 Z : impedance
 a_n : the n^{th} modal participation function
 d_n : the n^{th} modal damping coefficient
 $\{f\}$: a column matrix of point forces
 i : the imaginary coefficient, $\sqrt{-1}$
 K_n : a modal stiffness
 m_n : a modal mass
 t : time
 $\{v\}$: a column matrix of translation velocities
 Φ : phase
 Ω_n : the n^{th} damped resonant frequency
 α : the ratio of magnitudes of modal participation
 β : the ratio of normalized modal products

- ϵ : the participation of all modes but one in the admittance matrix or a displacement
 ξ_n : the n^{th} modal damping function
 η : the critical damping coefficient
 λ : the length of a shock cord
 $\{\phi^n\}$: the n^{th} mode shape
 ω : the frequency of excitation
 ω_n : the n^{th} resonant frequency
 $\{ \}$: a column matrix
 $[\]$: a row matrix
 $[\]$: a square matrix
 $[\]^{-1}$: an inverse matrix
 $[\]^T$: matrix transpose
 \leftarrow : a degree of freedom
 $\| \ \|$: the magnitude of a complex number

CHAPTER I

INTRODUCTION

The mechanical admittance* method or equivalently the mechanical impedance method is a means of characterizing the dynamic behavior of a structure by observing its dynamic behavior at a finite number of locations. In general, admittance and impedance are complex quantities defined for steady state, sinusoidal motion and are functions of the frequency of excitation. The admittance method is primarily experimental in nature and versatile in its applications.

Mechanical admittance embraces such diverse areas as acoustical transmission in structures to mode shape and resonant frequency determination. Rubin¹ uses admittance methods to reduce levels of engine noise transmitted to passenger compartments on commercial aircraft. Admittance methods are also applied to simple structures to determine resonant frequencies and transmission matrices.²

The fundamental difference between an admittance measurement and an impedance measurement is the displacement boundary conditions imposed on the structure during the measurement. For the purposes of this paper impedances are defined as the elements of the inverse of the admittance matrix. For an in depth treatment of the differences between admittance and impedance see reference 3.

* Admittance is synonymous with the term mobility.

This paper treats the problem of predicting the admittances for a composite structure from the measured admittances of the constituent substructures. In addition, mode shapes and resonant frequencies are estimated from the predicted admittances of the composite structure.

Chapter II deals with the mathematics involved in the admittance prediction technique. Chapter III is a brief description of the total experimental system and the function of the computer programs. Described in Chapter IV is the use of the total system for predicting the admittances, mode shapes and resonant frequencies for two simple composite structures.

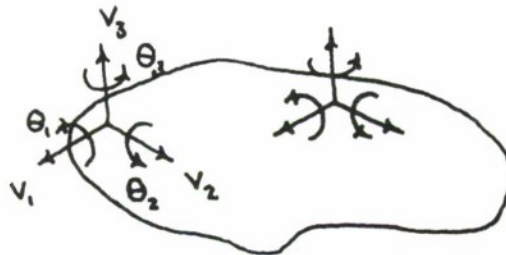
CHAPTER II

ANALYTIC BASIS2.1 The Mechanical Admittance and Mechanical Impedance of a Structure

For most structures of interest their low frequency dynamic behavior can be modeled by a lumped parameter or a finite element idealization. Attention is focused on linear elastic structures undergoing steady state, sinusoidal, forced excitation. This approach facilitates the derivation of general expressions for admittance and impedance.

$$\{Q\} = [M]\{\ddot{u}\} + [K]\{u\} \quad (2.1)$$

Equation 2.1 is the general equation of motion for a linear elastic structure. $\{Q\}$ is a column vector of the applied forces and moments. $\{u\}$ is a column vector of the resultant local displacements and rotations of the structure. The mass matrix, $[M]$, and the stiffness matrix, $[K]$, are square symmetric matrices of the same order as the number of degrees of freedom of the structure.



Schematic of the Degrees of Freedom of the Finite Element Idealization of a Continuous Structure

Figure 2.1

Equation 2.1 is rewritten for steady state, sinusoidal motion.

$$\{q\} e^{i\omega t} = [-\omega^2[M] + [K]]\{u\} e^{i\omega t} \quad (2.2)$$

$$\{Q\} = \{q\} e^{i\omega t} \quad (2.3)$$

$$\{u\} = \{u\} e^{i\omega t} \quad (2.4)$$

$$\{\ddot{u}\} = -\omega^2\{u\} e^{i\omega t} \quad (2.5)$$

If the mass and stiffness matrices are of order N , then there exist N homogeneous solutions, $\{\phi^n\}$, of equation 2.2

$$\{0\} = [-\omega_n^2[M] + [K]]\{\phi^n\} \quad (2.6)$$

The homogeneous solutions, $\{\phi^n\}$, exist only for a finite number of non-negative frequencies of motion, ω_n . ω_n is defined as the n^{th} resonant frequency of the structure. The column vector, $\{\phi^n\}$, is defined as the n^{th} mode shape of the structure.

In general the mode shapes are orthogonal to each other with respect to both the mass and stiffness matrices. Equations 2.7 and 2.8 are the definitions of orthogonality.

$$[\phi^j]^T [K] \{\phi^k\} = 0. \quad j \neq k \quad (2.7)$$

$$[\phi^j]^T [M] \{\phi^k\} = 0. \quad j \neq k \quad (2.8)$$

The resultant motion of the structure for forced excitation is assumed to be a linear combination of the mode shapes.

$$\{u\} = [\{\phi^1\} \{\phi^2\} \dots \{\phi^N\}] \{a\} = [\phi] \{a\} \quad (2.9)$$

The elements of the column vector, $\{a\}$, are the modal participation functions which are in general functions of frequency. If the modal participation functions are determined, then the forced response of the structure can be determined.

Substituting equation 2.9 into equation 2.2 and premultiplying both sides of equation 2.2 by $[\phi]^T$, equation 2.10 results.

$$[\phi]^T \{q\} e^{i\omega t} = [-\omega^2 [\phi]^T [M] [\phi] + [\phi]^T [K] [\phi]] \{a\} e^{i\omega t} \quad (2.10)$$

Invoking the orthogonality of the mode shapes with respect to the mass and stiffness matrices, equations 2.7 and 2.8, the mass and stiffness matrices are transformed into diagonal matrices.

$$[\phi]^T \{q\} = [-\omega^2 [M^*] + [K^*]] \{a\} \quad (2.11)$$

Each modal participation function can now be solved for algebraically.

$$a_n = \frac{[\phi^n]^T \{q\}}{(-\omega^2 m_n + K_n)} \quad (2.12)$$

$$m_n = m_{nn}^* \quad (2.13)$$

$$K_n = K_{nn}^* \quad (2.14)$$

Substituting the expression for the modal participation function, a_n , into equation 2.9 one can construct the forced response of the structure.

$$U_m = u_m e^{i\omega t} = \sum_{n=1}^N \frac{L\phi_n \{q\} \phi_m^n e^{i\omega t}}{(-\omega^2 m_n + K_n)} \quad (m=1,2,\dots,N) \quad (2.15)$$

For steady state, sinusoidal motion the resultant velocity at the m^{th} degree of freedom of the structure, V_m , can be expressed as a function of the resultant displacement, U_m , and the frequency of excitation, ω .

$$V_m = i\omega u_m e^{i\omega t} = \sum_{n=1}^N \frac{\frac{\omega}{m_n} L\phi_n \{q\} \phi_m^n e^{i\omega t}}{i(\omega^2 - \omega_n^2)} \quad (m=1,2,\dots,N) \quad (2.16)$$

$$\omega_n^2 = \frac{K_n}{m_n} \quad (2.17)$$

The admittance of a structure, $Y_{m\ell}(\omega)$, is defined as the ratio of the resultant velocity at the m^{th} degree of freedom of the structure to the force at the ℓ^{th} degree of freedom, assuming all other forces equal to zero.

$$Y_{m\ell}(\omega) = \frac{i\omega u_m e^{i\omega t}}{q_\ell e^{i\omega t}} = \sum_{n=1}^N \frac{\frac{\omega}{m_n} \phi_m^n \phi_\ell^n}{i(\omega^2 - \omega_n^2)} \quad (2.18)$$

This expression for admittance* is valid for applied moments and rotational velocities. Experimentally, admittances are usually measured only for point forces and trans-

* If the structure is modeled as a continuum, the expression for admittance is altered slightly. ϕ_m^n is replaced by the n^{th} continuous mode shape, ϕ^n , evaluated at the m^{th} degree of freedom of the structure.

lational velocities. For the remainder of the paper admittances are defined for point forces and translational velocities.

The admittances, $Y_{m_j}(\omega)$, are usually manipulated in matrix form, since admittances are measured on the structure at a finite number of points. Using superposition of velocities, an admittance matrix relating a column vector of point forces, $\{f\}$, to a column vector of translational velocities, $\{v\}$, can be formulated as in equation 2.19.

$$\begin{Bmatrix} v_1 \\ v_2 \\ \vdots \\ v_N \end{Bmatrix} = \begin{bmatrix} Y_{11}(\omega) & Y_{12}(\omega) & \dots & Y_{1N}(\omega) \\ Y_{21}(\omega) & Y_{22}(\omega) & \dots & \vdots \\ \vdots & \vdots & \ddots & \vdots \\ Y_{N1}(\omega) & \dots & \dots & Y_{NN}(\omega) \end{bmatrix} \begin{Bmatrix} f_1 \\ f_2 \\ \vdots \\ f_N \end{Bmatrix} \quad (2.19)$$

$$\{v\} = [Y]\{f\} \quad (2.20)$$

All of the admittances must be evaluated at the same frequency, ω , for the relationship to hold. Elements on the principal diagonal of the admittance matrix are the mutual admittances. All other elements of the admittance matrix are the cross admittances. Using equation 2.18 one can show that the admittance matrix, $[Y]$, is symmetric.

$$Y_{ml}(\omega) = \sum_{n=1}^N \frac{\omega}{m_n} \frac{\phi_m^n \phi_l^n}{i(\omega^2 - \omega_n^2)} = \sum_{n=1}^N \frac{\omega}{m_n} \frac{\phi_l^n \phi_m^n}{i(\omega^2 - \omega_n^2)} = Y_{lm}(\omega) \quad (2.21)$$

The p^{th} column of the admittance matrix, $Y_{j_p}(\omega)$ ($j=1,2,\dots,N$),

can be interpreted as the resultant velocities at the N degrees of freedom for a unit sinusoidal force at the p^{th} degree of freedom with no forces applied at the other degrees of freedom. Deleting the p^{th} row and column of the admittance matrix is equivalent to setting the p^{th} force equal to zero.

The inverse of the admittance matrix is defined as the mechanical impedance matrix, $[Z]$.

$$\{f\} = [Y]^{-1}\{v\} = [Z]\{v\} \quad (2.22)$$

Since the admittance matrix is symmetric, its inverse, the impedance matrix, is also symmetric. The elements on the principal diagonal of the impedance matrix are the mutual impedances. All other elements of the impedance matrix are the cross impedances.

$$\begin{pmatrix} f_1 \\ f_2 \\ \vdots \\ f_N \end{pmatrix} = \begin{bmatrix} Z_{11}(\omega) & Z_{12}(\omega) & \dots & Z_{1N}(\omega) \\ Z_{21}(\omega) & Z_{22}(\omega) & & \vdots \\ \vdots & & \ddots & \vdots \\ Z_{N1}(\omega) & \dots & \dots & Z_{NN}(\omega) \end{bmatrix} \begin{pmatrix} v_1 \\ v_2 \\ \vdots \\ v_N \end{pmatrix} \quad (2.23)$$

The p^{th} column of the impedance matrix, $Z_{jp}(\omega)$ ($j=1,2,\dots,N$), can be interpreted as the resultant forces at the N degrees of freedom for a unit sinusoidal displacement at the p^{th} degree of freedom with no velocity allowed at the other degrees of freedom. Deleting the p^{th} row and column of the impedance

matrix is equivalent to setting the p^{th} velocity equal to zero.

From a practical point of view, making admittance measurements on a structure is easier than making impedance measurements. To make an admittance measurement a force is applied at one degree of freedom and the resultant velocity is monitored at a degree of freedom with no velocity (displacement) boundary conditions imposed on the structure. To make an impedance measurement a velocity must be produced at one degree of freedom while the remaining degrees of freedom are held fixed. The reaction forces at the fixed degrees of freedom as well as the force at the point of excitation must be measured.

The stiffness matrix, $[K]$, and the flexibility matrix, $[C]$, used for static analysis of structures, are analogous to the impedance matrix, $[Z]$, and the admittance matrix, $[Y]$, respectively. Compare equations 2.22 and 2.20 with equations 2.24 and 2.25.

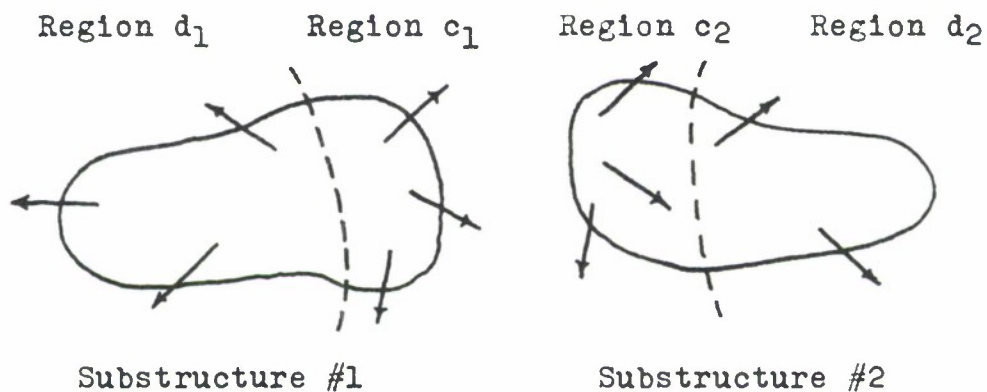
$$\{f^*\} = [K]\{x^*\} \quad (2.24)$$

$$\{x^*\} = [C]\{f^*\} \quad (2.25)$$

$\{f^*\}$ is a column vector of static loads and $\{x^*\}$ is a column vector of static displacements.

2.2 Assembling Substructures into a Composite Structure
Using Mechanical Impedance Notation

Assuming that admittance matrices have been measured for a number of substructures to be physically assembled into a composite structure, one can predict the properties of the composite structure by mathematically assembling the substructures using impedance notation. If the substructure admittance matrices are inverted to substructure impedance matrices, the substructure impedance matrices can be added to construct the composite structure impedance matrix.



Schematic of Substructures to be
 Assembled into a Composite Structure

Figure 2.2

Each substructure in Figure 2.2 is partitioned by a broken line. Those degrees of freedom that are to be joined to degrees of freedom on the other substructure are partitioned from the other degrees of freedom in the substructure.

The substructure impedance matrices in equations 2.26

and 2.27 are partitioned in an analogous manner. The elements of each impedance matrix corresponding to degrees of freedom that are to be joined to degrees of freedom on the other substructure are partitioned from the elements of the matrix corresponding to the other degrees of freedom of the substructure. Regions c_1 and c_2 in Figure 2.2 must have the same number of degrees of freedom to insure that $\{v_{c_1}\}$, $\{v_{c_2}\}$, $\{f_{c_1}\}$ and $\{f_{c_2}\}$ all have the same number of elements.

$$\begin{Bmatrix} f_{d_1} \\ f_{c_1} \end{Bmatrix} = \begin{bmatrix} Z_{d_1 d_1} & Z_{d_1 c_1} \\ Z_{c_1 d_1} & Z_{c_1 c_1} \end{bmatrix} \begin{Bmatrix} v_{d_1} \\ v_{c_1} \end{Bmatrix} \quad (2.26)$$

$$\begin{Bmatrix} f_{c_2} \\ f_{d_2} \end{Bmatrix} = \begin{bmatrix} Z_{c_2 c_2} & Z_{c_2 d_2} \\ Z_{d_2 c_2} & Z_{d_2 d_2} \end{bmatrix} \begin{Bmatrix} v_{c_2} \\ v_{d_2} \end{Bmatrix} \quad (2.27)$$

Equations 2.26 and 2.27 are separated into four matrix equations for the forces in the four regions of Figure 2.2.

$$\{f_{d_1}\} = [Z_{d_1 d_1}]\{v_{d_1}\} + [Z_{d_1 c_1}]\{v_{c_1}\} \quad (2.28)$$

$$\{f_{c_1}\} = [Z_{c_1 d_1}]\{v_{d_1}\} + [Z_{c_1 c_1}]\{v_{c_1}\} \quad (2.29)$$

$$\{f_{c_2}\} = [Z_{c_2 c_2}]\{v_{c_2}\} + [Z_{c_2 d_2}]\{v_{d_2}\} \quad (2.30)$$

$$\{f_{d_2}\} = [Z_{d_2 c_2}]\{v_{c_2}\} + [Z_{d_2 d_2}]\{v_{d_2}\} \quad (2.31)$$

Using equilibrium between internal forces, $\{f_{c_1}\}$, $\{f_{c_2}\}$ and applied forces, $\{f_c\}$, equations 2.29 and 2.30 can be added to give the applied forces in region c of the composite structure.

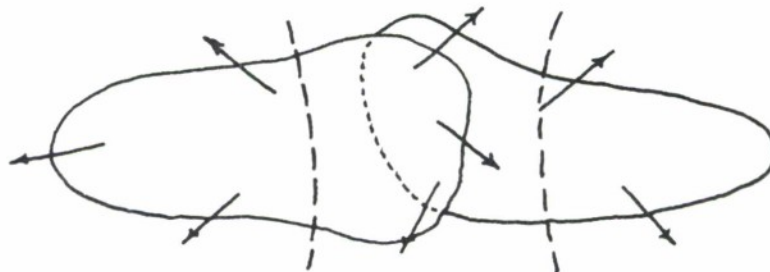
$$\{f_c\} - \{f_{c_1}\} - \{f_{c_2}\} = \{0\} \quad (2.32)$$

$$\{f_c\} = \{f_{c_1}\} + \{f_{c_2}\} = [Z_{c,d_1}]\{v_{d_1}\} \quad (2.33)$$

$$+ [Z_{c,c_1}]\{v_{c_1}\} + [Z_{c_2,c_2}]\{v_{c_2}\} + [Z_{c_2,d_2}]\{v_{d_2}\}$$

Region d₁

Region c

Region d₂

Schematic of Assembled Composite Structure

Figure 2.3

Invoking compatibility of velocities, equation 2.34, at the degrees of freedom common to both substructures in region c, equation 2.33 can be reduced to equation 2.35.

$$\{v_{c_1}\} = \{v_{c_2}\} = \{v_c\} \quad (2.34)$$

$$\{f_c\} = [Z_{c,d_1}]\{v_{d_1}\} + [Z_{c,c_1} + Z_{c_2,c_2}]\{v_c\} + [Z_{c_2,d_2}]\{v_{d_2}\} \quad (2.35)$$

The impedance matrix for the composite structure is

constructed from equations 2.28, 2.31 and 2.35.

$$\begin{Bmatrix} f_{d_1} \\ f_c \\ f_{d_2} \end{Bmatrix} = \begin{bmatrix} Z_{d_1 d_1} & Z_{d_1 c_1} & 0 \\ Z_{c_1 d_1} & Z_{c_1 c_1} + Z_{c_2 c_2} & Z_{c_2 d_2} \\ 0 & Z_{d_2 c_2} & Z_{d_2 d_2} \end{bmatrix} \begin{Bmatrix} v_{d_1} \\ v_c \\ v_{d_2} \end{Bmatrix} \quad (2.36)$$

Since the measured admittances for the substructures are valid only for translational velocities, the substructure impedance matrices are valid only for translational velocities. Consequently, at the points of attachment of the substructures one can insure the compatibility of translational velocities only, equation 2.34. It follows that the attachment points of the first substructure are allowed to rotate independently from the attachment points of the second substructure. As a result of this limitation in assembling substructures analytically, composite structures that have large rotational impedances at the attachment points of their constituent substructures will not be accurately modeled by the composite structure impedance matrix.

Displacement boundary conditions are imposed on the composite structure by operations on the composite structure's impedance matrix. One makes the velocity of the p^{th} degree of freedom zero by deleting the p^{th} row and column of the impedance matrix. Since impedances are available just for translational velocities, only translational

velocities of the composite structure can be made zero.

After the displacement boundary conditions are imposed on the composite structure impedance matrix, it is inverted to the composite structure admittance matrix. The resonant frequencies and accompanying mode shapes of the composite structure are estimated from the predicted admittance matrix for the composite structure as shown in section 2.4.

2.3 The Effect of Damping on Resonant Frequencies and Admittances

In section 2.1 the resonant frequencies of a structure are defined as ω_n and the mode shapes are defined as $\{\phi^n\}$. As the frequency of excitation, ω , tends to ω_n , the forced response of the structure tends to infinity where the ratio of the response at one degree of freedom of the structure to the response at another degree of freedom is defined by $\{\phi^n\}$. The property of damping exhibited in most real structures changes the definition of resonant frequencies. Consequently, damping affects the magnitude and phase of an admittance at or near a resonant frequency of the structure.

To facilitate the discussion of damping it is assumed that the damping present in the structure is modal damping. Each mode is assumed to exhibit damping independently of the damping of other modes.

This form of damping is represented mathematically by introducing a diagonal damping matrix into equation 2.11.

$$\{f\} e^{i\omega t} = \left[-\omega^2 [M^*] + i\omega [C^*] + [K^*] \right] \{a\} e^{i\omega t} \quad (2.37)$$

The modal participation functions, a_n , are solved for in the same manner as in section 2.1.

$$a_n = \frac{\frac{1}{m_n} [\phi^n] \{f\}}{i\omega c_n(\omega) + (\omega_n^2 - \omega^2)} \quad (2.38)$$

$$\zeta_n(\omega) = \frac{C_{nn}^*(\omega)}{m_{nn}} \quad (2.39)$$

$\zeta_n(\omega)$ is the modal damping coefficient. For viscous damping $\zeta_n(\omega)$ is $d_n \omega_n$. For hysteretic damping $\zeta_n(\omega)$ is of the form shown in equation 2.40.

$$\zeta_n(\omega) = \frac{d_n \omega_n^2}{\omega} \quad (2.40)$$

The admittance of a structure with modal damping is given in equation 2.41.

$$Y_{ml}(\omega) = \sum_{n=1}^N \frac{\frac{\omega}{m_n} \phi_m^n \phi_l^n}{\zeta_n(\omega) \omega + i(\omega^2 - \omega_n^2)} = \sum_{n=1}^N \frac{\frac{\omega}{m_n} \phi_l^n \phi_m^n}{\zeta_n(\omega) \omega + i(\omega^2 - \omega_n^2)} = Y_{lm}(\omega) \quad (2.41)$$

The admittance matrix for a structure with modal damping is symmetric. Consequently, the impedance matrix for a structure with modal damping is also symmetric.

The poles of equation 2.41 are the damped resonant frequencies of the structure, Ω_n , and are, in general, complex numbers.

$$\zeta_n(\Omega_n) \Omega_n + i(\Omega_n^2 - \omega_n^2) = 0. \quad (2.42)$$

The damped resonant frequencies can be solved for explicitly for viscous damping, equation 2.43, and hysteretic damping, equation 2.44.

$$\Omega_n = \omega_n \left(1 - \frac{d_n^2}{4}\right)^{1/2} + i \omega_n \frac{d_n}{2} \quad \zeta_n(\omega) = d_n \omega_n \quad (2.43)$$

$$\Omega_n = \omega_n (1 + i d_n)^{1/2} \quad \zeta_n(\omega) = \frac{d_n \omega_n^2}{\omega} \quad (2.44)$$

The damping coefficient, d_n , is much less than one for low frequencies of excitation in most structures. For hysteretic and viscous damping d_n^{-1} is the Q_n^* factor or the resonant quality of the n^{th} mode. For the remainder of the chapter Q_n^* is assumed to be 50.

If the frequency of excitation is near the j^{th} undamped resonant frequency, ω_j , the j^{th} term in equation 2.41 is most representative of the structure's admittance.

$$Y_{m\ell}(\omega) = \frac{\frac{\omega}{m_j} \phi_m^j \phi_\ell^j}{\mathcal{G}_j(\omega)\omega + i(\omega^2 - \omega_j^2)} + \epsilon_{m\ell} \quad (2.45)$$

$$\epsilon_{m\ell} = \sum_{\substack{n=1 \\ n \neq j}}^N \frac{\frac{\omega}{m_n} \phi_m^n \phi_\ell^n}{\mathcal{G}_n(\omega)\omega + i(\omega^2 - \omega_n^2)} \quad (2.46)$$

$\epsilon_{m\ell}$ represents the participation of all modes but the j^{th} for $\omega \approx \omega_j$. The admittance matrix for the structure excited near the j^{th} undamped resonant frequency is given in equation 2.47.

$$\begin{Bmatrix} v_1 \\ v_2 \\ \vdots \\ v_N \end{Bmatrix} = \frac{\omega}{m_j} \frac{1}{\mathcal{G}_j(\omega)\omega + i(\omega^2 - \omega_j^2)} \begin{bmatrix} \phi_1^j \phi_1^j & \phi_1^j \phi_2^j & \dots & \phi_1^j \phi_N^j \\ \phi_2^j \phi_1^j & \phi_2^j \phi_2^j & & \vdots \\ \vdots & & \ddots & \vdots \\ \phi_N^j \phi_1^j & \dots & \dots & \phi_N^j \phi_N^j \end{bmatrix} \begin{Bmatrix} f_1 \\ f_2 \\ \vdots \\ f_N \end{Bmatrix} \\ + \begin{bmatrix} \epsilon_{11} & \epsilon_{12} & \dots & \epsilon_{1N} \\ \epsilon_{21} & \epsilon_{22} & & \vdots \\ \vdots & & \ddots & \vdots \\ \epsilon_{N1} & \dots & \dots & \epsilon_{NN} \end{bmatrix} \begin{Bmatrix} f_1 \\ f_2 \\ \vdots \\ f_N \end{Bmatrix} \quad (2.47)$$

$$\{v\} = [Y]\{f\} = [J]\{f\} + [e]\{f\} \quad (2.48)$$

If all ϵ_{mq} are zero for $\omega \approx \omega_j$, then the matrix, $[J]$, is equal to the admittance matrix. All of the elements of $[J]$ are either in phase, 0 radians, or out of phase, π radians, with respect to each other for $\omega \approx \omega_j$. All the elements of $[J]$ have a local maximum at one frequency of excitation. This frequency is the real part of the damped resonant frequency defined in equation 2.42.

In general the participation of all modes except the j^{th} , ϵ_{mq} , is not zero for $\omega \approx \omega_j$. It follows that the elements of the admittance matrix, $J_{mq} + \epsilon_{mq}$, will not have their local maxima at exactly the same frequency for $\omega \approx \omega_j$. In addition the elements of the admittance matrix are not exactly in or out of phase with respect to each other for any frequency of excitation.

2.4 Estimating Resonant Frequencies and Mode Shapes for Composite Structures from Predicted Admittance Data

The predicted admittances of a structure are the normalized levels of the forced response. The levels of the forced response are normalized by the magnitudes of the applied forces.

Equation 2.47 is representative of the behavior of an admittance matrix at or near the j^{th} undamped resonant frequency of the structure.

$$\begin{aligned}
 \begin{pmatrix} v_1 \\ v_2 \\ \vdots \\ v_N \end{pmatrix} &= \frac{\frac{\omega}{m_j}}{q_j(\omega)\omega + i(\omega^2 - \omega_j^2)} \begin{bmatrix} \phi_1^j \phi_1^j & \phi_1^j \phi_2^j & \cdots & \phi_1^j \phi_N^j \\ \phi_2^j \phi_1^j & \phi_2^j \phi_2^j & & \vdots \\ \vdots & & \ddots & \vdots \\ \phi_N^j \phi_1^j & & & \phi_N^j \phi_N^j \end{bmatrix} \begin{pmatrix} f_1 \\ f_2 \\ \vdots \\ f_N \end{pmatrix} \\
 &+ \begin{bmatrix} \epsilon_{11} & \epsilon_{12} & \cdots & \epsilon_{1N} \\ \epsilon_{21} & \epsilon_{22} & & \vdots \\ \vdots & & \ddots & \vdots \\ \epsilon_{N1} & & & \epsilon_{NN} \end{bmatrix} \begin{pmatrix} f_1 \\ f_2 \\ \vdots \\ f_N \end{pmatrix} \quad (2.47)
 \end{aligned}$$

$$\{v\} = [Y]\{f\} = [J]\{f\} + [e]\{f\} \quad (2.48)$$

If the participation of all modes except the j^{th} , ϵ_{mj} , is very small compared to the participation of the j^{th} mode, then one can predict the j^{th} resonant frequency and mode shape from the admittance matrix. The frequency at which the elements of the admittance matrix have their j^{th} local maximum is the j^{th} resonant frequency. The rows and columns

of the admittance matrix are proportional to the j^{th} mode shape, $\{\phi^j\}$, for $\omega \approx \omega_j$.

In general there are two cases where the participation of all modes except the j^{th} is not small compared to the participation of the j^{th} mode for $\omega \approx \omega_j$. First, if an admittance is predicted for a degree of freedom at or near a node of the j^{th} mode shape, that admittance is more representative of the participation of modes other than the j^{th} . Second, if two resonant frequencies of the structure are close together, the admittance matrix is representative of the participation of both modes at either resonant frequency.

If an element of the admittance matrix corresponds to a degree of freedom near a node of the j^{th} mode shape and is dominated by the participation of modes other than the j^{th} , then that element will not have a well defined maximum in magnitude in the region of the j^{th} resonant frequency.

$$E_{m\ell} = \sum_{\substack{n=1 \\ n \neq j}}^N \frac{\frac{\omega}{m_n} \phi_m^n \phi_\ell^n}{Q_n(\omega)\omega + i(\omega^2 - \omega_n^2)} \quad (2.46)$$

The expression for the participation of all modes but the j^{th} , $E_{m\ell}$, does not have any poles near ω_j . Therefore, there is no local maximum in magnitude of $E_{m\ell}$ for $\omega \approx \omega_j$.

If two resonant frequencies of the structure are close together, then the admittance can be approximated by the participation of only those two modes for frequencies of excitation near the two resonant frequencies.

$$Y_{m\ell}(\omega) = \frac{\frac{\omega}{m_j} \phi_m^j \phi_\ell^j}{\zeta_j(\omega)\omega + i(\omega^2 - \omega_j^2)} + \frac{\frac{\omega}{m_p} \phi_m^p \phi_\ell^p}{\zeta_p(\omega)\omega + i(\omega^2 - \omega_p^2)} \quad (2.49)$$

Evaluating the admittance at ω_j one can solve for values of $\frac{\omega_p}{\omega_j}$ such that the magnitude of the participation of the p^{th} mode is α of the participation of the j^{th} mode at the j^{th} resonant frequency.

$$\alpha \left\| \frac{\frac{\omega_j}{m_j} \phi_m^j \phi_\ell^j}{\zeta_j(\omega_j)\omega_j + i(\omega_j^2 - \omega_j^2)} \right\| = \left\| \frac{\frac{\omega_j}{m_p} \phi_m^p \phi_\ell^p}{\zeta_p(\omega_j)\omega_j + i(\omega_j^2 - \omega_p^2)} \right\| \quad (2.50)$$

The damping for both modes is assumed to be viscous.

$$\zeta_j(\omega) = d_j \omega_j = 2\eta_j \omega_j \quad (2.51)$$

$$\zeta_p(\omega) = d_p \omega_p = 2\eta_p \omega_p \quad (2.52)$$

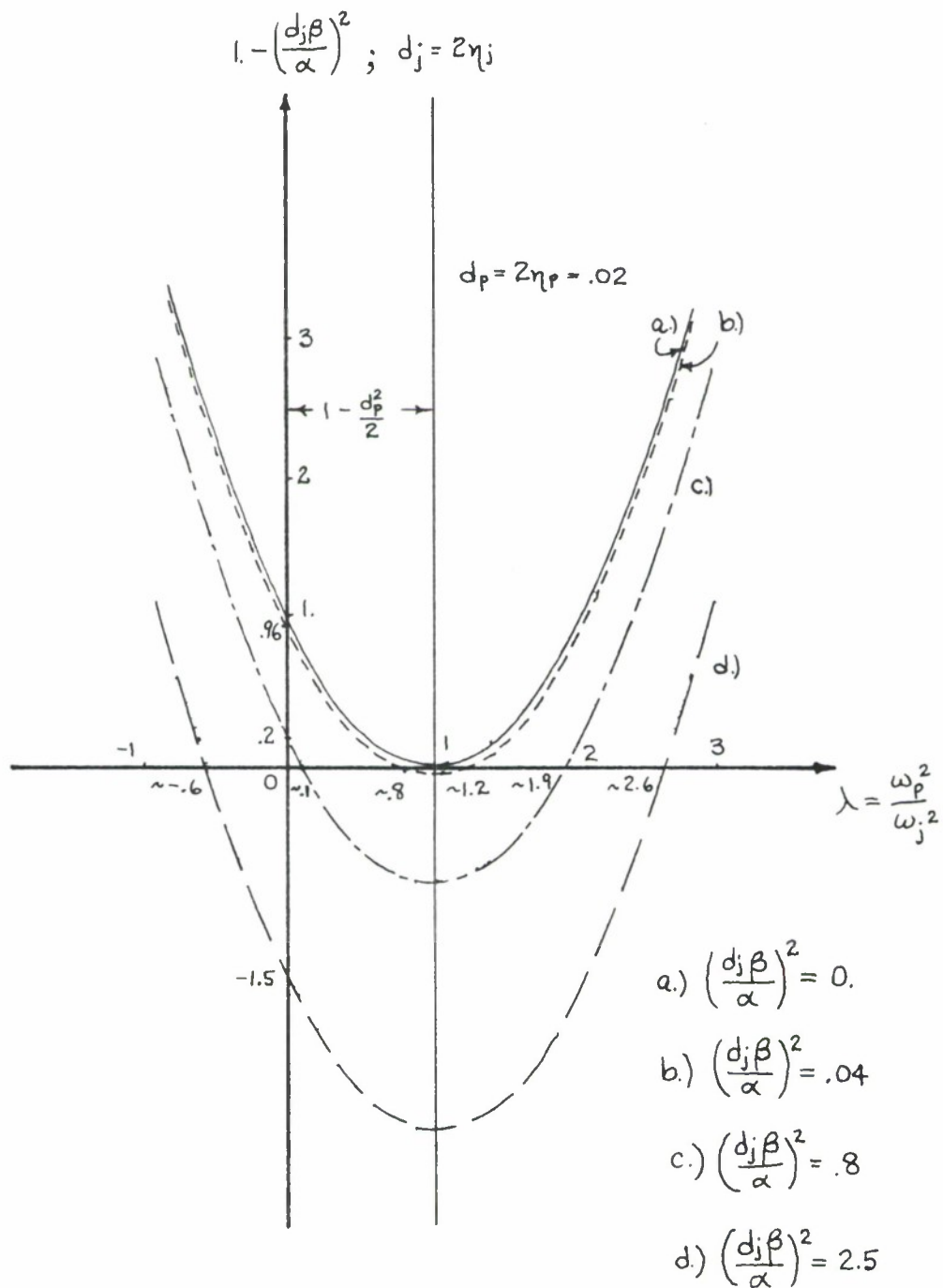
η is the ratio of the damping of the mode to critical damping for that mode. The ratio of the normalized modal products for the p^{th} and j^{th} modes is β .

$$\beta = \frac{\frac{1}{m_p} \phi_m^p \phi_\ell^p}{\frac{1}{m_j} \phi_m^j \phi_\ell^j} \quad (2.53)$$

Substituting equations 2.51, 2.52 and 2.53 into equation 2.50 one can solve for values of $\frac{\omega_p}{\omega_j}$.

$$\lambda^2 - (2 - 4\eta_p^2)\lambda + 1 - 4\frac{\eta_j^2 \beta^2}{\alpha^2} = 0. \quad (2.54)$$

$$\lambda = \frac{\omega_p^2}{\omega_j^2} \quad (2.55)$$



Plots of Equation 2.54 for Different Values of the Parameters d_n , α , and β

Figure 2.4

Figure 2.4 shows plots of equation 2.54 for different values of the parameters, d_n , α and β . Assuming the modal damping coefficients d_n are .02, the ratio of the normalized modal products β is 1.0 and α is .1, the roots of equation 2.54 are given in equations 2.56 and 2.57.

$$\lambda = \frac{\omega_p^2}{\omega_j^2} \approx 1.2 \quad (2.56)$$

$$\lambda = \frac{\omega_p^2}{\omega_j^2} \approx .8 \quad (2.57)$$

Thus, if $\frac{\omega_p^2}{\omega_j^2}$ is greater than .8 and less than 1.2, the participation of the p^{th} mode at the j^{th} resonant frequency is greater than 10%. If $\frac{\omega_p^2}{\omega_j^2}$ is less than .8 or greater than 1.2, the participation of the p^{th} mode at the j^{th} resonant frequency is less than 10%.

The participation of the p^{th} mode affects the phase of the admittance at the j^{th} resonant frequency. The two modal participation terms in equation 2.49 are treated as vectors in the complex plane.

$$Y_{m\ell}(\omega) = \frac{\frac{\omega}{m_j} \phi_m^j \phi_\ell^j}{\zeta_j(\omega)\omega + i(\omega^2 - \omega_j^2)} + \frac{\frac{\omega}{m_p} \phi_m^p \phi_\ell^p}{\zeta_p(\omega)\omega + i(\omega^2 - \omega_p^2)} \quad (2.49)$$

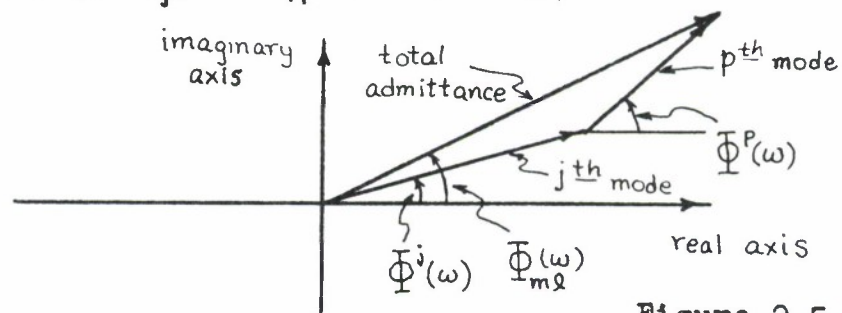


Figure 2.5

The Modal Participation Vectors of the p^{th} and j^{th} Modes in the Complex Plane

The phases of the two modal participation vectors evaluated at ω_j are given in equations 2.58 through 2.61.

$$\Phi_{m\ell}^j(\omega_j) = -\tan^{-1} \left\{ \frac{\omega_j^2 - \omega_j^2}{\mathcal{Q}_j(\omega_j)\omega_j} \right\} = 0 \quad \Phi_m^j \Phi_\ell^j > 0 \quad (2.58)$$

$$\Phi_{m\ell}^j(\omega_j) = \pi - \tan^{-1} \left\{ \frac{\omega_j^2 - \omega_j^2}{\mathcal{Q}_j(\omega_j)\omega_j} \right\} = \pi \quad \Phi_m^j \Phi_\ell^j < 0 \quad (2.59)$$

$$\Phi_{m\ell}^p(\omega_j) = -\tan^{-1} \left\{ \frac{\omega_j^2 - \omega_p^2}{\mathcal{Q}_p(\omega_j)\omega_j} \right\} \quad \Phi_m^p \Phi_\ell^p > 0 \quad (2.60)$$

$$\Phi_{m\ell}^p(\omega_j) = \pi - \tan^{-1} \left\{ \frac{\omega_j^2 - \omega_p^2}{\mathcal{Q}_p(\omega_j)\omega_j} \right\} \quad \Phi_m^p \Phi_\ell^p < 0 \quad (2.61)$$

If M_j is the magnitude of the participation of the j^{th} mode and M_p is the magnitude of the participation of the p^{th} mode, the phase of the admittance at the j^{th} resonant frequency is given in equations 2.62 and 2.63.

$$\Phi_{m\ell}(\omega_j) = \tan^{-1} \left\{ \frac{M_p \sin \Phi^p(\omega_j)}{M_j + M_p \cos \Phi^p(\omega_j)} \right\} \quad \Phi^j(\omega_j) = 0 \quad (2.62)$$

$$\Phi_{m\ell}(\omega_j) = \pi + \tan^{-1} \left\{ \frac{-M_p \sin \Phi^p(\omega_j)}{-M_j + M_p \cos \Phi^p(\omega_j)} \right\} \quad \Phi^j(\omega_j) = \pi \quad (2.63)$$

The participation of the p^{th} mode affects the phase of the admittance most when $\Phi^p(\omega_j) = \pm \frac{\pi}{2}$.

$$\Phi_{m\ell}(\omega_j) = \tan^{-1} \left\{ \pm \frac{M_p}{M_j} \right\} = \tan^{-1} \{ \pm \alpha \} \approx \pm \alpha \quad \Phi^j(\omega_j) = 0 \quad (2.64)$$

$$\Phi_{m\ell}(\omega_j) = \pi + \tan^{-1} \left\{ \pm \frac{M_p}{M_j} \right\} = \tan^{-1} \{ \pm \alpha \} \approx \pi \pm \alpha \quad \Phi^j(\omega_j) = \pi \quad (2.65)$$

The effect of the p^{th} mode on the phase of the admittance at the j^{th} resonant frequency is at most α radians. α is defined in equation 2.50.

Assuming that the j^{th} resonant frequency is not close to other resonant frequencies of the structure, the j^{th} mode shape is calculated from the maximum values of the magnitudes for the admittances near the j^{th} resonant frequency. An element of the admittance matrix that does not have a local maximum in magnitude for $\omega \approx \omega_j$ and is dominated by the participation of modes other than the j^{th} is not used to calculate the j^{th} mode shape.

The signs of the components of the mode shape vector, $\{\phi^j\}$, are determined by the relative phases of the admittances at the j^{th} resonant frequency. Unfortunately, the admittance data is available only for a finite number of frequencies which may not coincide with the exact resonant frequencies of the composite structure. However, as long as the participation of modes other than the j^{th} is small for

$\omega \approx \omega_j$, the relative phases of the admittances at the j^{th} resonant frequency are approximately the same as their relative phases near the j^{th} resonant frequency.

The matrix $[J]$ is approximately equal to the admittance matrix at the j^{th} resonant frequency if the participation of modes other than the j^{th} is small.* Equations 2.66 and 2.67 give the phases of elements of the matrix $[J]$.

* See equation 2.48.

$$\Phi_{m\ell}(\omega) = -\tan^{-1} \left\{ \frac{\omega^2 - \omega_j^2}{\ell_j(\omega)\omega} \right\} \quad \phi_m^j \phi_\ell^j > 0 \quad (2.66)$$

$$\Phi_{m\ell}(\omega) = \pi - \tan^{-1} \left\{ \frac{\omega^2 - \omega_j^2}{\ell_j(\omega)\omega} \right\} \quad \phi_m^j \phi_\ell^j < 0 \quad (2.67)$$

The relative phases of the elements of the matrix $[J]$ are 0 or π radians for all frequencies of excitation, ω . These relative phases determine the signs of the components of the j^{th} mode shape vector, $\{\phi^j\}$ and are approximately equal to the relative phases of the admittances at the j^{th} resonant frequency of the structure.

CHAPTER III

The Mechanical Admittance Measurement and Prediction System

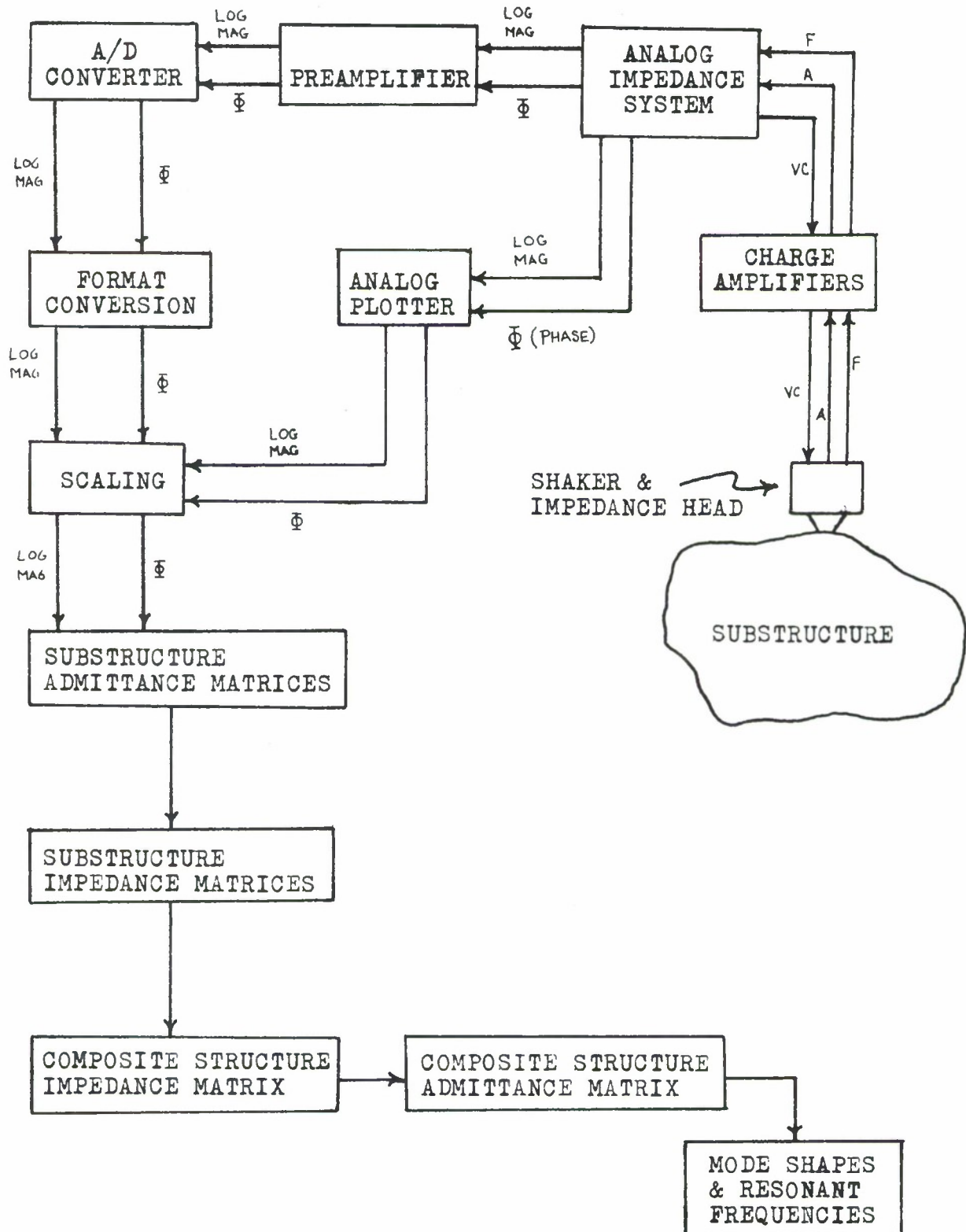
The primary function of the measurement and prediction system is to predict the admittances of a composite structure from admittance measurements made on the constituent substructures. The admittance measurements for the substructures are made in analog form and then converted to digital form to construct the substructure admittance matrices. The substructure admittance matrices are used to calculate the composite structure admittance matrix.

The admittances of a substructure are constructed from force and acceleration measurements made on the substructure. The force and acceleration measured are resultants of a force input to the structure generated by an electromagnetic shaker. The resultant force imparted to the substructure is measured by a very stiff, lightweight strain gauge mounted between the shaker and the substructure. The resultant acceleration is measured by an accelerometer mounted behind the strain gauge or at some location on the substructure.

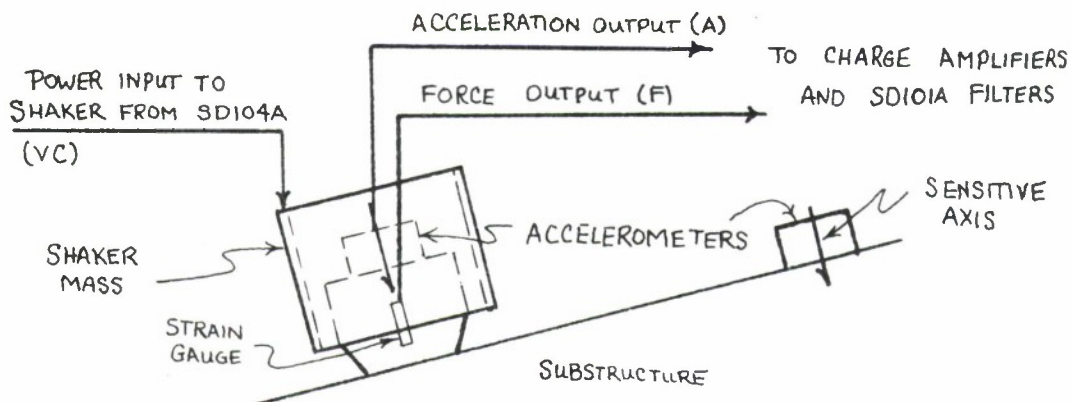
The force input to the structure generated by the shaker is proportional to the deflection of the strain gauge. Because the alloy in which the strain gauge is embedded is stiff and lightweight, the acceleration measured behind the strain gauge is the local acceleration of the substructure

The Mechanical Admittance Measurement and Prediction System

Figure 3.1



in front of the strain gauge except at very high frequencies of excitation.⁴



Schematic of Shaker and Impedance Head

Figure 3.2

A strain gauge with an accelerometer mounted behind it as in Figure 3.2 is referred to as an "impedance head". The device used in the following experiments is a Z602 impedance head made by Wilcoxon Research. The shaker is a F3 "wrap around" shaker also made by Wilcoxon Research.*

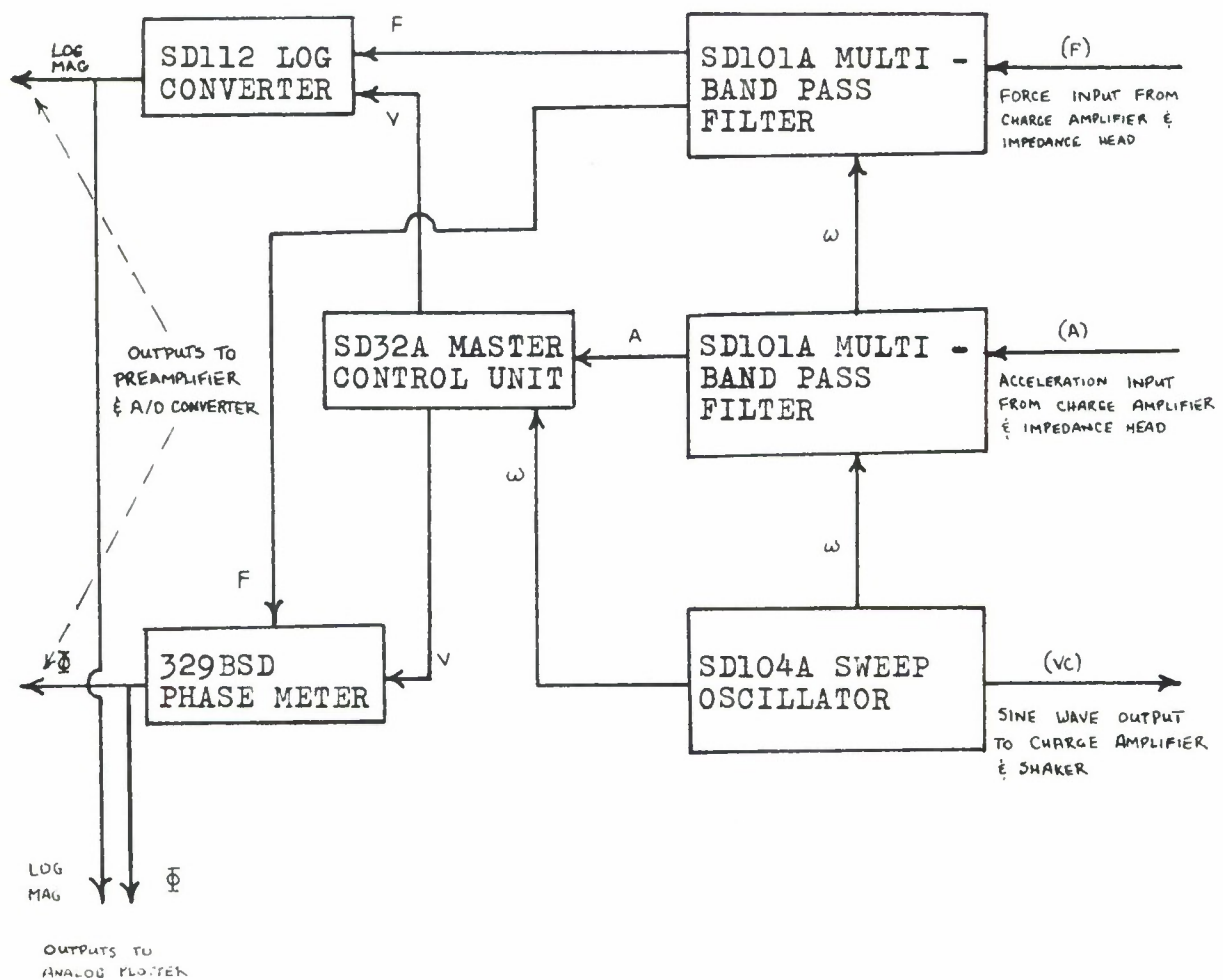
The admittances of a substructure are measured over a finite frequency range by varying the frequency of the input to the shaker from the SD104A sweep oscillator. The resultant force and acceleration signals are amplified and put into the analog impedance equipment. These signals are band pass filtered before they are used to calculate the \log_{10} (magnitude) and phase of the measured admittance.

Each SD101A filter is made of many band pass filters.

* The specifications for these instruments appear in reference 5.

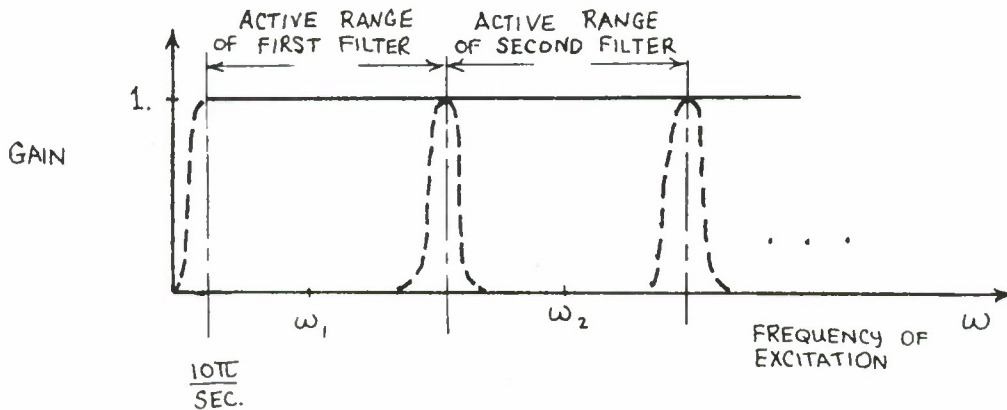
Schematic of the SD1002B-33 Automatic Mechanical Impedance System* in the Mechanical Admittance Mode

Figure 3.3



* For a complete description of the SD1002B-33 Automatic Mechanical Impedance System, see reference 7.

Each band pass filter has a unique center frequency and is active over a finite frequency range that includes its center frequency. The active ranges of the band pass filters cover a broad frequency range, 5 Hz. to 10 kilo-Hz., and they do not overlap.



Schematic of the Transfer Function of a
SD101A Filter in the Frequency Domain

Figure 3.4

Only one band pass filter is active for a given frequency of excitation generated by the SD104A sweep oscillator. The resultant force and acceleration signals generated by the impedance head should have the same frequency as the frequency of excitation for the shaker generated by the SD104A. If other frequencies are present in the force and acceleration signals outside the band of the active filter, they are eliminated from the signals. This filtering is done to make more accurate phase and magnitude calculations for the admittance.

The filtered acceleration signal is divided by the frequency of excitation and shifted in phase by $-\frac{\pi}{2}$ radians

to yield the velocity of the substructure. The velocity signal and the filtered force signal are used to calculate the admittance of the structure. The SD112 log converter generates a voltage proportional to the \log_{10} (magnitude) of the admittance. The 329BSD phase meter generates a voltage proportional to the phase of the admittance.

The voltages proportional to phase and \log_{10} (magnitude) are plotted on a 136AR Hewlett Packard X Y₁ Y₂ Recorder. These voltages are also preamplified and put into a Radiation analog-to-digital (A/D) converter.

The A/D converter has one analog input channel and generates 12 bit digital words from the input voltage. The input voltage range is -2 volts to +2 volts. With a twelve bit register the A/D converter can generate 4096 different numbers corresponding to the four volt input range or roughly one number for every millivolt input.

The outputs from the analog impedance system are typically 50 millivolts. To achieve any accuracy in the digital data these signals must be preamplified before they are put into the A/D converter. After making a preliminary frequency sweep to establish the maximum and minimum values of the voltage output from the impedance system, the bias and gain are adjusted on the preamplifier to take full advantage of the A/D converter's four volt input range.

* For a complete description of the Radiation A/D converter see reference 6.



The SD1002B-33 Automatic Mechanical
Impedance System and Charge Amplifiers

Figure 3.5

A second frequency sweep is made to sample and convert the amplified analog signal from the impedance system, and the digital data is stored on magnetic tape.

Because the A/D converter has only one input channel the \log_{10} (magnitude) and the phase of the admittance are converted on two separate frequency sweeps*. The digital data is converted in format from 12 bit words to 32 bit words that the IBM 360 computer can understand. Each 12 bit word is padded with 20 extra bits without changing the value of the number in the word by the computer program CONVERT.

The digital data is scaled from the analog plots made on the Hewlett Packard recorder. Two values of the phase or magnitude from a plot, P_1 and P_2 , are compared to two values of the digital data, D_1 and D_2 , for corresponding frequencies of excitation. The gain and bias introduced into the digital data by the preamplifier are calculated.

$$\text{GAIN} = \frac{(D_2 - D_1)}{(P_2 - P_1)} \quad (3.1)$$

$$\text{BIAS} = \frac{D_1(P_2 - P_1)}{(D_2 - D_1)} - P_1 \quad (3.2)$$

* If a two track tape recorder is available it is better to record phase and \log_{10} (magnitude) on the same frequency sweep and then to put the analog signals into the A/D converter one track at a time.

All of the digital data corresponding to the analog plot is scaled using the calculated gain and bias. D_m is the unscaled value of the digital data for the m^{th} frequency of excitation. S_m is the scaled value of D_m .

$$S_m = -(\text{BIAS}) + (\text{GAIN})^{-1} D_m = P_1 - \frac{P_2 - P_1}{D_2 - D_1} (D_m - D_1) \quad (3.3)$$

This scaling process must be done twice for each admittance, once for phase and once for magnitude. All scaling is done by the computer program SCALE.

The scaled data is used to construct the substructure admittance matrix for the sampled frequencies of excitation. After all of the substructure admittance matrices are constructed they are inverted* to substructure impedance matrices. The substructure impedance matrices are assembled into the composite structure impedance matrix. All matrix inversion and assembling is done by the computer program ADMIT.

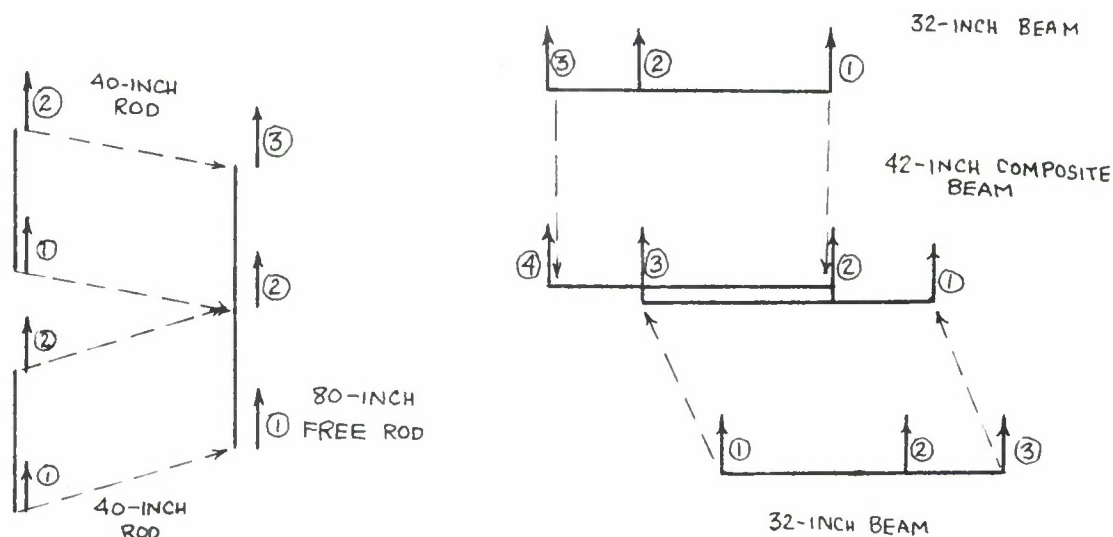
The mode shapes and resonant frequencies of the composite structure are estimated from the admittances of the composite structure as shown in section 2.4.

* The method of matrix inversion is described in Appendix A.

CHAPTER IV

EXPERIMENTAL RESULTS4.1 Introduction to Experimental Results

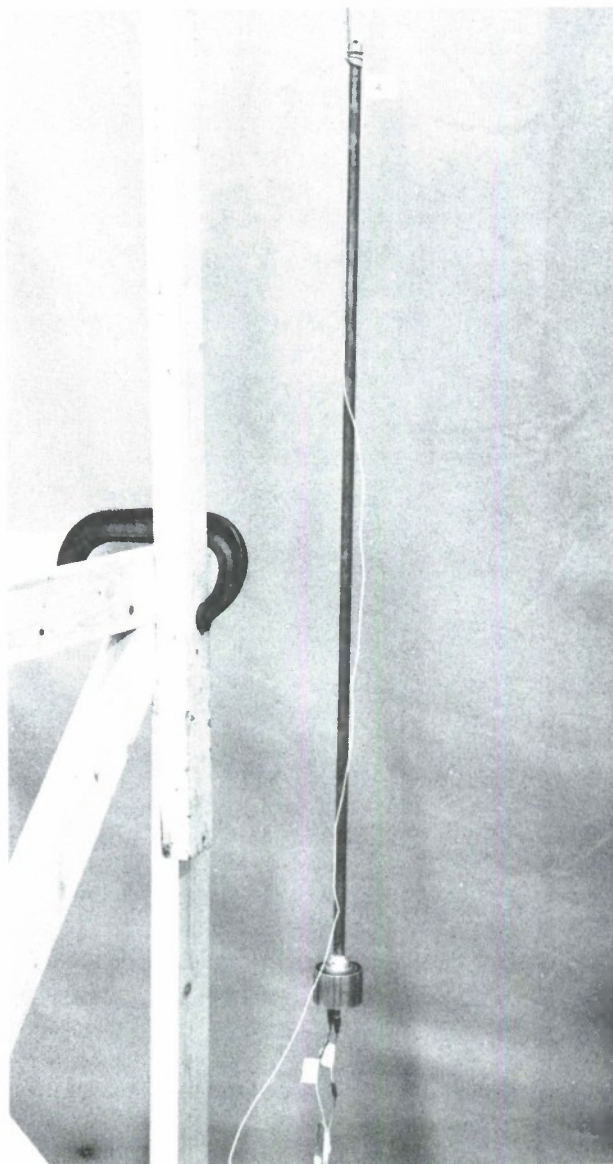
The admittance measurement and prediction system is applied to two composite structures. The first composite structure is an 80-inch free rod assembled from two 40-inch free rods. The second composite structure is two 32-inch beams pinned together.



Schematic of Assembling Two Composite Structures
from Their Constituent Substructures

Figure 4.1

Admittance measurements are made only on the substructures. The "predicted" admittances are the admittances of the composite structure predicted by the computer program ADMIT. The "calculated" admittances are generated by analytical modal models of the structures and are used only for comparison with the "measured" and "predicted" admittances.



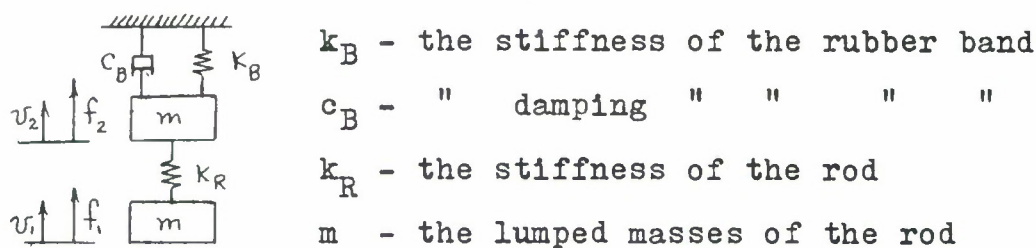
Measuring the Cross Admittance
of a 40-Inch Steel Rod

Figure 4.2

4.2 The Effects of the Suspension System, Impedance Head and Shaker on the Measured Admittances of a 40-Inch Free Rod

A rubber band suspension system shown in Figure 4.2 is used to simulate a free rod for frequencies of excitation, ω , well above the resonant frequency of the suspension system. The resonant frequency of the rod and rubber band ensemble is 1.2 c.p.s., which is well below the lowest frequency for which admittance measurements are made on the rod ($\frac{\omega}{2\pi} \geq 50$ c.p.s.).

In order to estimate the effect of the rubber band on the measured admittances, the rod and rubber band are modeled as a two degree of freedom, lumped parameter system. See Figure 4.3. Because the model has only two degrees of freedom it will be representative of the system for frequencies of excitation up to, and including, the second resonant frequency of the rod and rubber band ensemble. However, this two-degree of freedom model will give some indication of the effects of the rubber band suspension system on the measured admittances of the rod.



The Lumped Parameter Model of the Rubber
Band and Rod Ensemble

Figure 4.3

The impedance matrix, $[Z]$, of the ensemble is written as the sum of a mass matrix, $[M]$, a damping matrix, $[C]$, and a stiffness matrix, $[K]$. The damping in the rod is assumed to be zero; the damping in the rubber band is assumed to be viscous.

$$[Z] = i\omega [M] + [C] + (i\omega)^{-1} [K] \quad (4.1)$$

$$[Z] = i\omega \begin{bmatrix} m & 0 \\ 0 & m \end{bmatrix} + \begin{bmatrix} 0 & 0 \\ 0 & C_B \end{bmatrix} + (i\omega)^{-1} \begin{bmatrix} K_R & -K_R \\ -K_R & K_R + K_B \end{bmatrix} \quad (4.2)$$

The admittance matrix for the system is found by inverting the impedance matrix. The elements of the admittance matrix are shown in equations 4.5 through 4.7, and the parameters w_1 and w_2 are defined in equations 4.3 and 4.4.

$$w_1 = \left\{ \frac{K_B}{2m} \right\}^{1/2} \quad (4.3)$$

$$w_2 = \left\{ \frac{2K_R}{m} \right\}^{1/2} \quad (4.4)$$

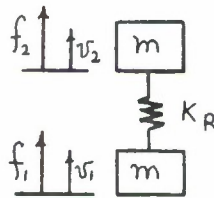
$$Y_{11}(\omega) = \frac{\frac{\omega}{m} \left[\frac{\omega^2}{w_2^2} - \frac{1}{2} \left(1 + \frac{w_1^2}{w_2^2} \right) \right] + \frac{C_B \omega^2}{m^2 w_2^2}}{i \left(\frac{\omega^4}{w_2^2} - \omega^2 - 2\omega^2 \frac{w_1^2}{w_2^2} - w_1^2 \right) + \left(\frac{\omega^2}{w_2^2} - \frac{1}{2} \right) \frac{\omega}{m} C_B} \quad (4.5)$$

$$Y_{21}(\omega) = \frac{-\frac{1}{2} \frac{\omega}{m}}{i \left(\frac{\omega^4}{w_2^2} - \omega^2 - 2\omega^2 \frac{w_1^2}{w_2^2} - w_1^2 \right) + \left(\frac{\omega^2}{w_2^2} - \frac{1}{2} \right) \frac{\omega}{m} C_B} \quad (4.6)$$

$$Y_{22}(\omega) = \frac{\frac{\omega}{m} \left[\frac{\omega^2}{w_2^2} - \frac{1}{2} \left(1 + \frac{w_1^2}{w_2^2} \right) \right]}{i \left(\frac{\omega^4}{w_2^2} - \omega^2 - 2\omega^2 \frac{w_1^2}{w_2^2} - w_1^2 \right) + \left(\frac{\omega^2}{w_2^2} - \frac{1}{2} \right) \frac{\omega}{m} C_B} \quad (4.7)$$

$$\frac{W_1^2}{W_2^2} = \frac{K_B}{4K_R} \quad (4.8)$$

For comparison the admittances of a free rod, modeled by a spring and two masses, are given in equations 4.9 and 4.10.



Lumped Parameter Model of a Free Rod

Figure 4.4

$$Y_{11}(\omega) = Y_{22}(\omega) = \frac{\frac{\omega}{m} \left(\frac{\omega^2}{\omega_2^{*2}} - \frac{1}{2} \right)}{i \left(\frac{\omega^4}{\omega_2^{*2}} - \omega^2 \right)} \quad (4.9)$$

$$Y_{12}(\omega) = Y_{21}(\omega) = \frac{-\frac{1}{2} \frac{\omega}{m}}{i \left(\frac{\omega^4}{\omega_2^{*2}} - \omega^2 \right)} \quad (4.10)$$

ω_2^* is the first resonant frequency of the free rod for elastic motion.

$$\omega_2^* = \omega_2 = \left\{ \frac{2K_R}{m} \right\}^{1/2} \quad (4.11)$$

If $\frac{W_1^2}{W_2^2}$ and C_B are zero, the admittances for the rod and rubber band ensemble are equal to the admittances for the free rod. For the system shown in Figure 4.2, $\frac{W_1^2}{W_2^2}$ is 5.6×10^{-7} and c_B is $.403 \frac{\text{lb.-sec.}}{\text{in.}}$. This value of c_B is 17% of critical damping.

$\frac{W_1^2}{W_2^2}$ is derived using a calculated stiffness for the rod and a measured stiffness for the rubber band.

$$K_R = \frac{AE}{L} = 1.47 \times 10^5 \frac{\text{lb.}}{\text{in.}} \quad (4.12)$$

$$K_B = .33 \frac{\text{lb.}}{\text{in.}} \quad (4.13)$$

$$\frac{W_1^2}{W_2^2} = \frac{K_B}{4K_R} = 5.6 \times 10^{-7} \quad (4.14)$$

c_B is calculated by observing the rate of decay of motion for the rod and rubber band ensemble oscillating in its first mode.

By substituting the values of $\frac{W_1^2}{W_2^2}$ and c_B into equations 4.5 through 4.7 the effect of the rubber band support system on the admittances is determined.

$$Y_{11}(\omega) = \frac{\frac{\omega}{m} \left[\frac{\omega^2}{W_2^2} - \frac{1}{2} (1 + 11.2 \times 10^{-7}) \right] + \frac{\omega^2}{m^2 W_2^2} .403}{i \left(\frac{\omega^4}{W_2^2} - \omega^2 - \omega^2 (11.2 \times 10^{-7}) - W_1^2 \right) + \left(\frac{\omega^2}{W_2^2} - \frac{1}{2} \right) \frac{\omega}{m} .403} \quad (4.15)$$

$$Y_{12}(\omega) = Y_{21}(\omega) = \frac{-\frac{1}{2} \frac{\omega}{m}}{i \left(\frac{\omega^4}{W_2^2} - \omega^2 - \omega^2 (11.2 \times 10^{-7}) - W_1^2 \right) + \left(\frac{\omega^2}{W_2^2} - \frac{1}{2} \right) \frac{\omega}{m} .403} \quad (4.16)$$

$$Y_{22}(\omega) = \frac{\frac{\omega}{m} \left[\frac{\omega^2}{W_2^2} - \frac{1}{2} (1 + 11.2 \times 10^{-7}) \right]}{i \left(\frac{\omega^4}{W_2^2} - \omega^2 - \omega^2 (11.2 \times 10^{-7}) - W_1^2 \right) + \left(\frac{\omega^2}{W_2^2} - \frac{1}{2} \right) \frac{\omega}{m} .403} \quad (4.17)$$

If ω , the circular frequency of excitation, is much greater than w_1 , the admittances are affected very slightly by the stiffness of the rubber band. At the first resonant

frequency of the free rod, ω_2 , the magnitudes of the admittances are very sensitive to the values of c_B .

The additional mass of the shaker and impedance head attached to the lower end of the rod, Figure 4.2, also affects the measured admittances. The impedance matrix for a two-degree of freedom, free rod with the mass of the shaker and impedance head, m_s , added is given in equation 4.18.

$$[Z] = (i\omega) \begin{bmatrix} m+m_s & 0 \\ 0 & m \end{bmatrix} + (i\omega)^{-1} \begin{bmatrix} K_R & -K_R \\ -K_R & K_R \end{bmatrix} \quad (4.18)$$

The expression for the first resonant frequency for elastic motion is $\hat{\omega}_1$.

$$\hat{\omega}_1 = \left\{ \frac{2K_R}{m} \right\}^{1/2} \left\{ \frac{1 + \frac{m_s}{2m}}{1 + \frac{m_s}{m}} \right\}^{1/2} = \omega_2^* \left\{ \frac{1 + \frac{m_s}{2m}}{1 + \frac{m_s}{m}} \right\}^{1/2} \quad (4.19)$$

If $\frac{m_s}{m} \ll 1$, the resonant frequency of the rod with the shaker and impedance head attached is not appreciably affected by the additional mass, m_s . However, $\frac{m_s}{m}$ for the ensemble in Figure 4.2 is .786, and the first resonant frequency for the 40-inch rod with the shaker and impedance head attached should be significantly lower than ω_2^* .

$$\hat{\omega}_1 = .886 \omega_2^* \quad (4.20)$$

By modeling the rod with more degrees of freedom it can be

shown that the higher resonant frequencies of the rod will be lower if the shaker and impedance head are attached.

The magnitude and phase of the measured admittances are affected appreciably by the mass of the shaker and impedance head when $\omega = \omega_2^*$.

$$Y_{11}(\omega) = \frac{\left(\frac{\omega^2}{\omega_2^{*2}} - \frac{1}{2}\right)}{i\omega m \left[\left(\frac{\omega^2}{\omega_2^{*2}} - 1\right) + \frac{m_s}{m} \left(\frac{\omega^2}{\omega_2^{*2}} - \frac{1}{2}\right)\right]} \quad (4.21)$$

$$Y_{11}(\omega_2^*) = (i\omega_2^* m_s)^{-1} \quad (4.22)$$

By comparing the measured admittances for the total ensemble of the rod, rubber band, shaker and impedance head to admittances calculated for a 40-inch free rod, the effects of the suspension system, shaker and impedance head on the measured admittances are evident. See Figures 4.6 through 4.9.

The calculated admittances are generated by solving equation 4.23 for a free rod.

$$E \frac{\partial^2 u}{\partial x^2} + \rho \frac{\partial^2 u}{\partial t^2} = 0. \quad (4.23)$$

$$\frac{\partial u(0)}{\partial x} = 0. \quad (4.24)$$

$$\frac{\partial u(L)}{\partial x} = 0. \quad (4.25)$$



Schematic of
a Free Rod
Figure 4.5

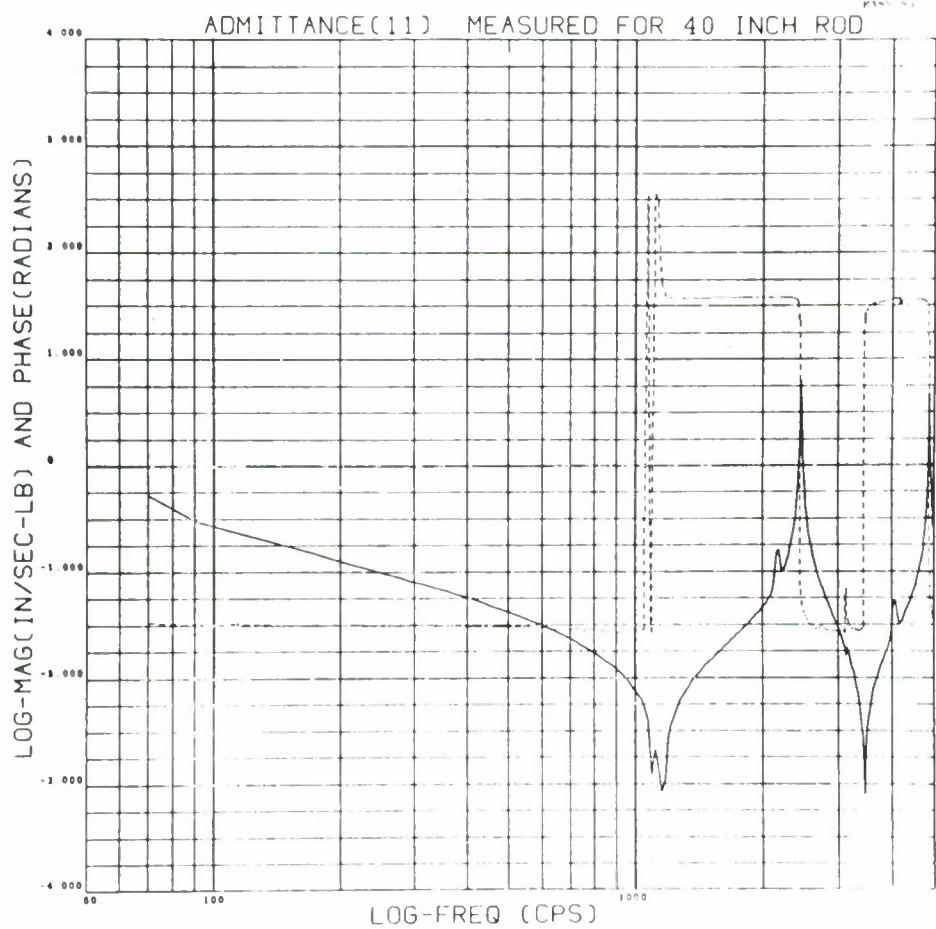


Figure 4.6

Note: On all admittance plots of the type shown above, the broken line is phase and the solid line is magnitude.

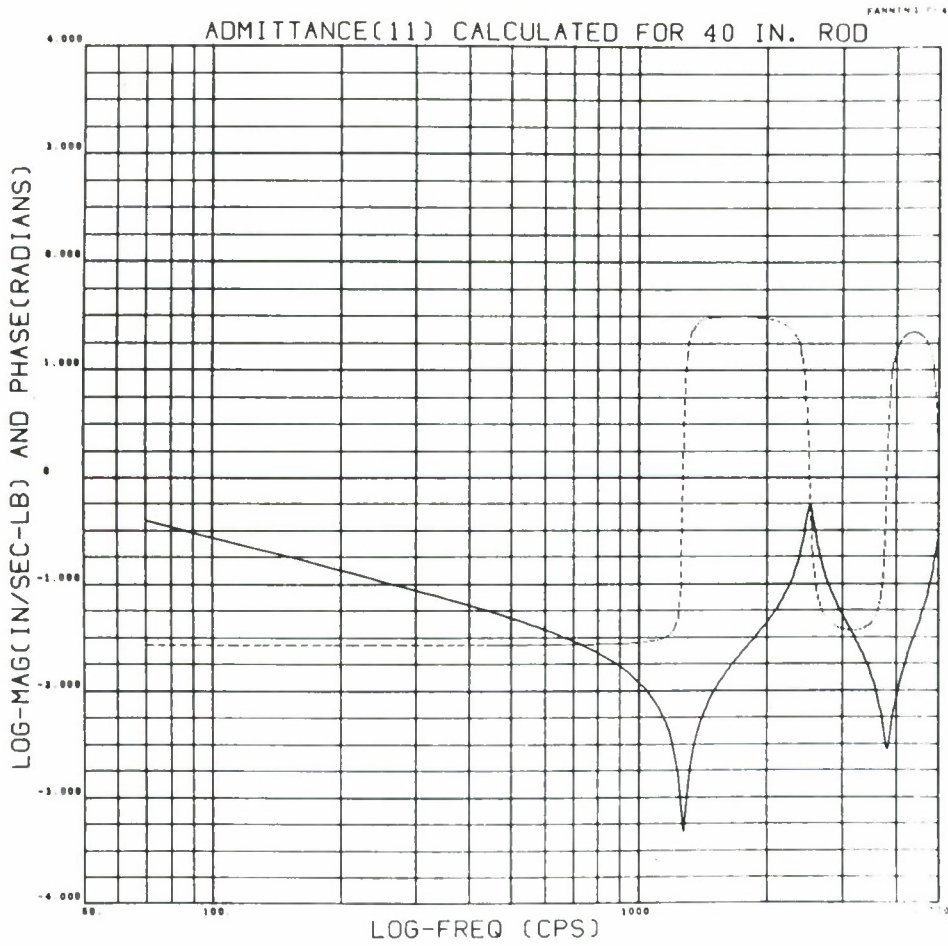


Figure 4.7

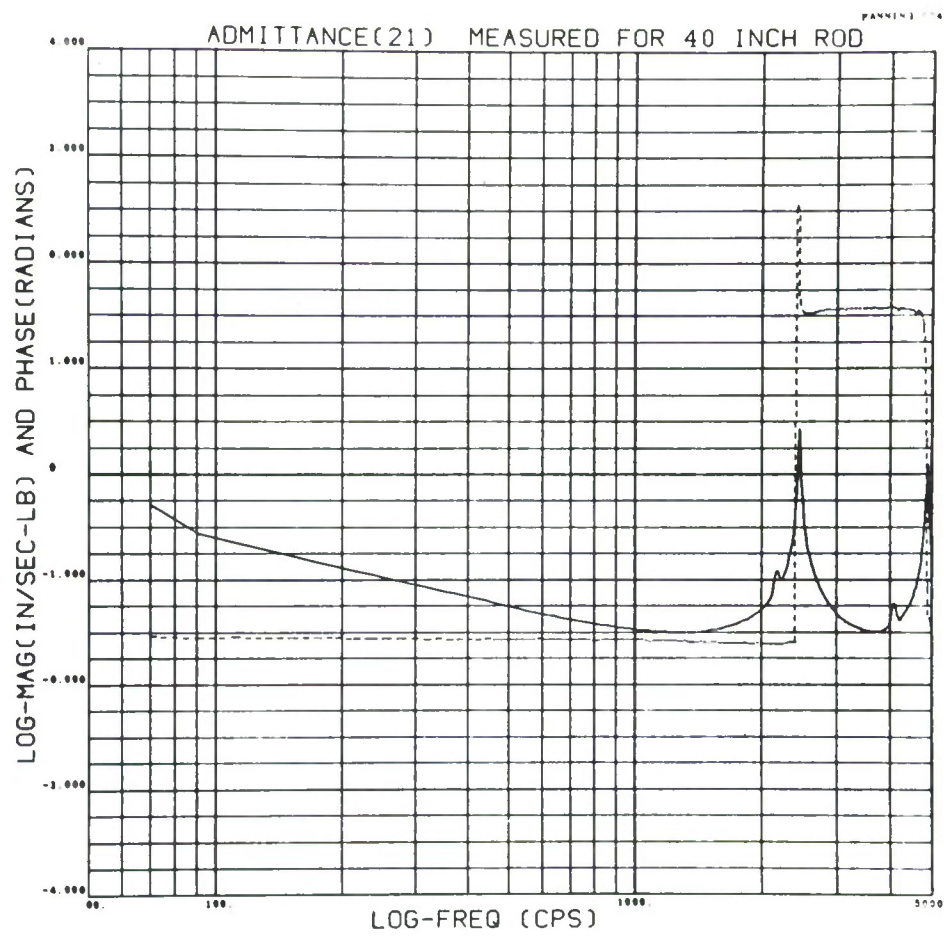


Figure 4.8

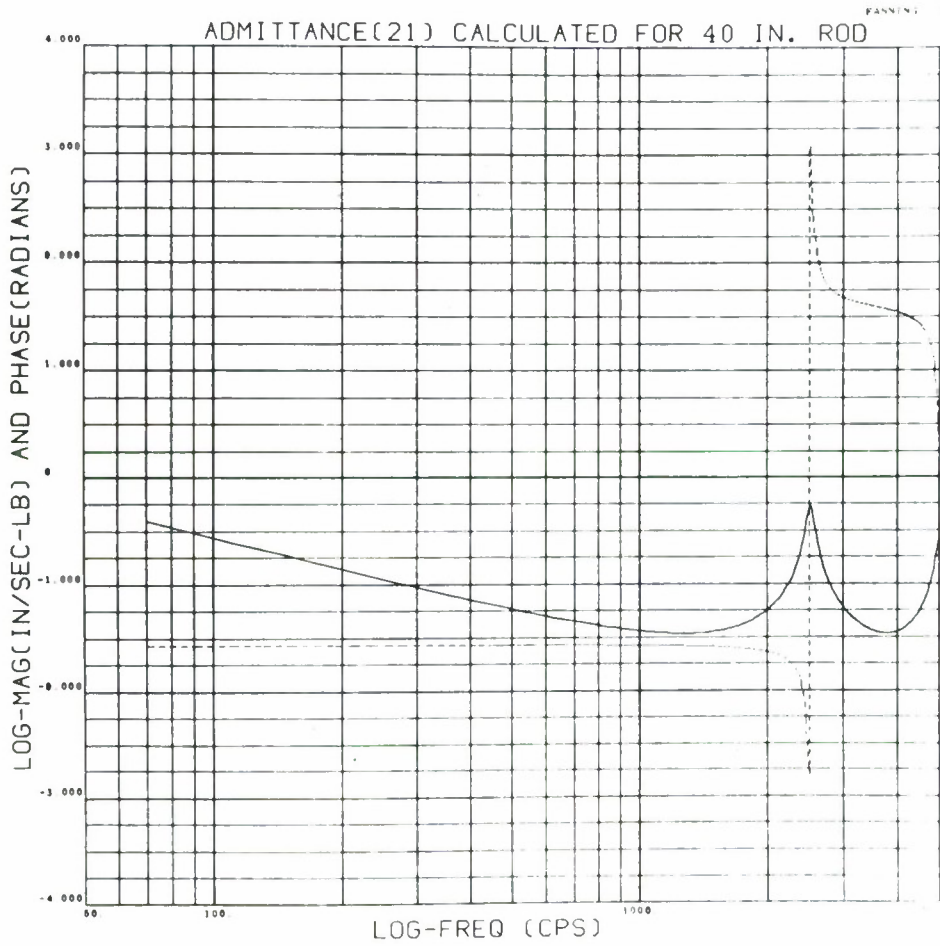


Figure 4.9

u is the axial displacement of the rod and is a function of the location, x , and time, t .

| | |
|----------------------------|---|
| E - Young's Modulus | 29.8×10^6 psi |
| A - Cross Sectional Area | $.198$ in ² |
| ρ - Density | $.284$ $\frac{\text{lb.}}{\text{in}^3}$ |
| L - Length | $40.$ in. |

Properties of a 40-Inch
Steel Rod
Table 4.1

The solutions to equation 4.23 incorporating the boundary conditions in equations 4.24 and 4.25 are given in equation 4.26.

$$\phi^n(x) = \cos \frac{n\pi x}{L} \quad (4.26)$$

The admittances of the free rod are constructed in a manner similar to the method used in section 2.1.

$$Y_{m\ell}(\omega) = \sum_{n=0}^{\infty} \frac{\frac{\omega}{m_n} \phi^n(x_m) \phi^n(x_\ell)}{\zeta_n(\omega) \omega + i(\omega^2 - \omega_n^2)} \quad (4.27)$$

$$m_n = \int_0^L \rho A \cos^2 \frac{n\pi x}{L} dx \quad (4.28)$$

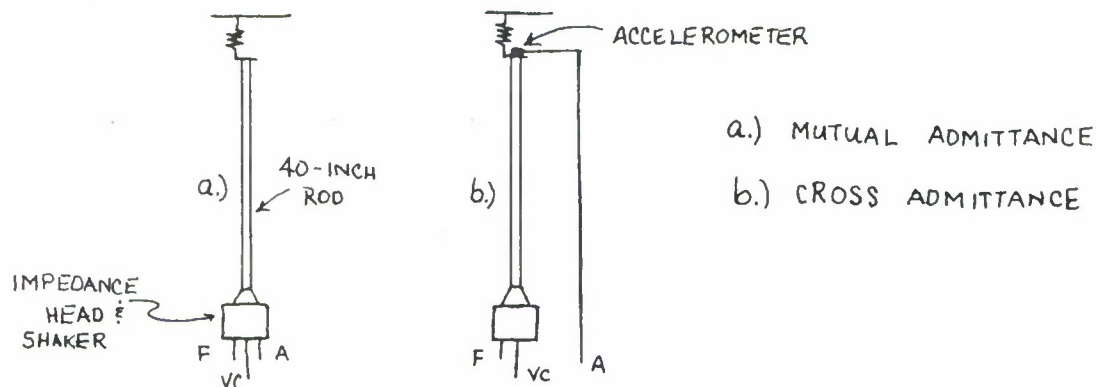
$$\omega_n = \frac{n\pi}{L} \left(\frac{E}{\rho} \right)^{1/2} \quad (4.29)$$

$$\zeta_n(\omega) = .02 \omega_n \quad (4.30)$$

The admittances of the free rod are calculated for 242 frequencies from 50 c.p.s. to 5000 c.p.s. These are the same frequencies at which the measured admittances are sampled and scaled. The damping is equivalent to 1% of critical damping.

4.3 Predicting the Admittances, Resonant Frequencies and Mode Shapes for an 80-Inch Free Rod

The mutual and cross admittances for a 40-inch free rod are measured as shown in Figure 4.10. The mutual admittance is measured using the accelerometer in the impedance head. The cross admittance is measured using an accelerometer attached to the top end of the rod.

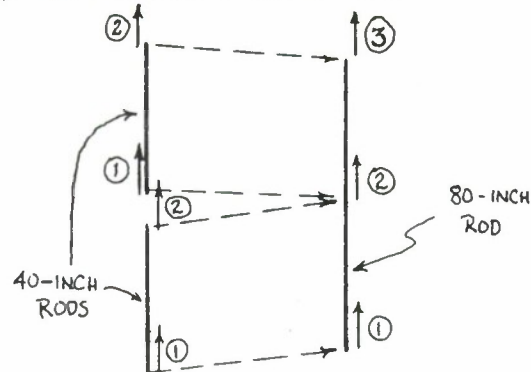


Schematic of Measuring the Admittances for a 40-Inch Rod

Figure 4.10

Having measured the mutual and cross admittances is sufficient to construct two identical, 2×2 , substructure admittance matrices. The mutual admittance of one end of the rod is the same as the mutual admittance of the other end; the cross admittances are the same due to symmetry in the admittance matrix. Assuming that admittance measurements made on one 40-inch rod should not, in principle, differ from admittance measurements made on a second 40-inch rod, two identical substructure admittance matrices are constructed from admittance measurements made on one 40-inch rod.

The two admittance matrices for the 40-inch rod substructures are inverted to substructure impedance matrices. The substructure impedance matrices are assembled, as shown in section 2.2, to yield the impedance matrix of the composite structure, an 80-inch free rod.



Schematic of Assembling an 80-Inch Rod from Two 40-Inch Rods

Figure 4.11

The impedance matrix for the 80-inch rod is inverted to the composite structure admittance matrix. The four unique elements of the composite structure admittance matrix are plotted as a function of the frequency of excitation in Figures 4.12 through 4.15. Figures 4.16 through 4.19 are calculated admittances for an 80-inch free rod. These admittances are calculated using equation 4.27. The damping in the calculated admittances is 1% of critical damping.

The admittance matrix of the composite structure is used to estimate resonant frequencies and mode shapes of the composite structure as shown in section 2.4. The predicted mode shapes for the 80-inch rod that have corresponding resonant frequencies that coincide with resonant frequencies of the substructures are not accurate. See Table 4.2.

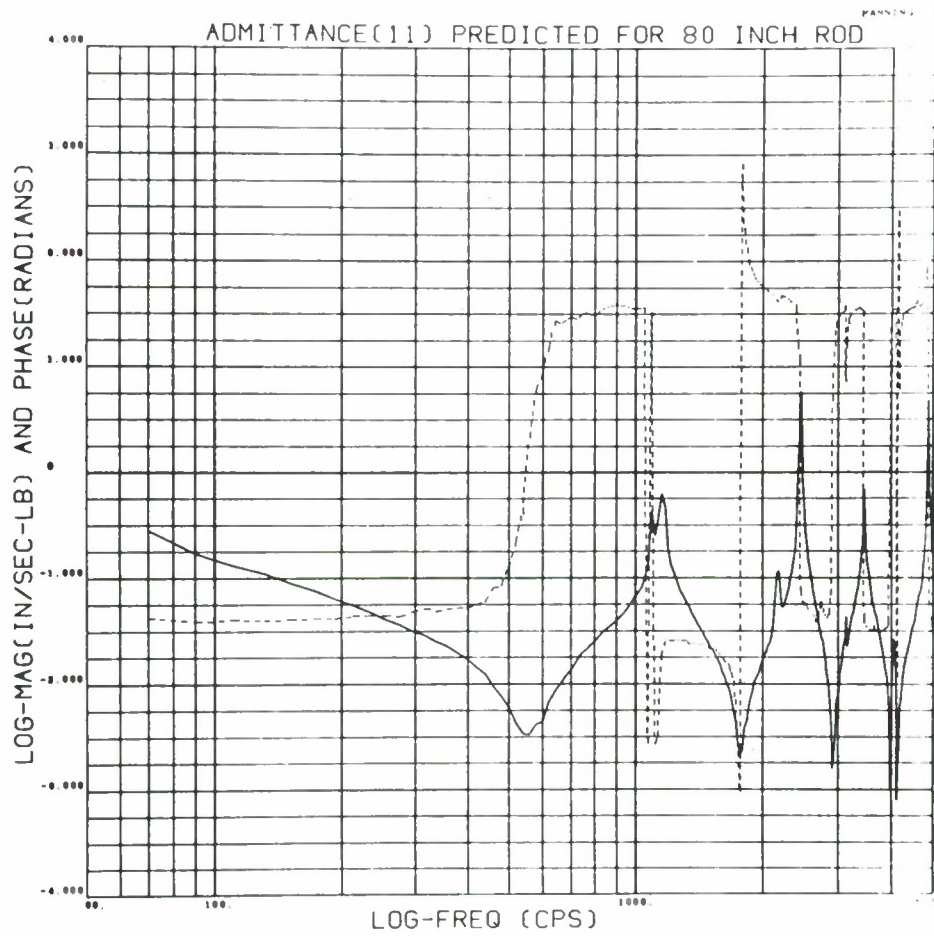


Figure 4.12

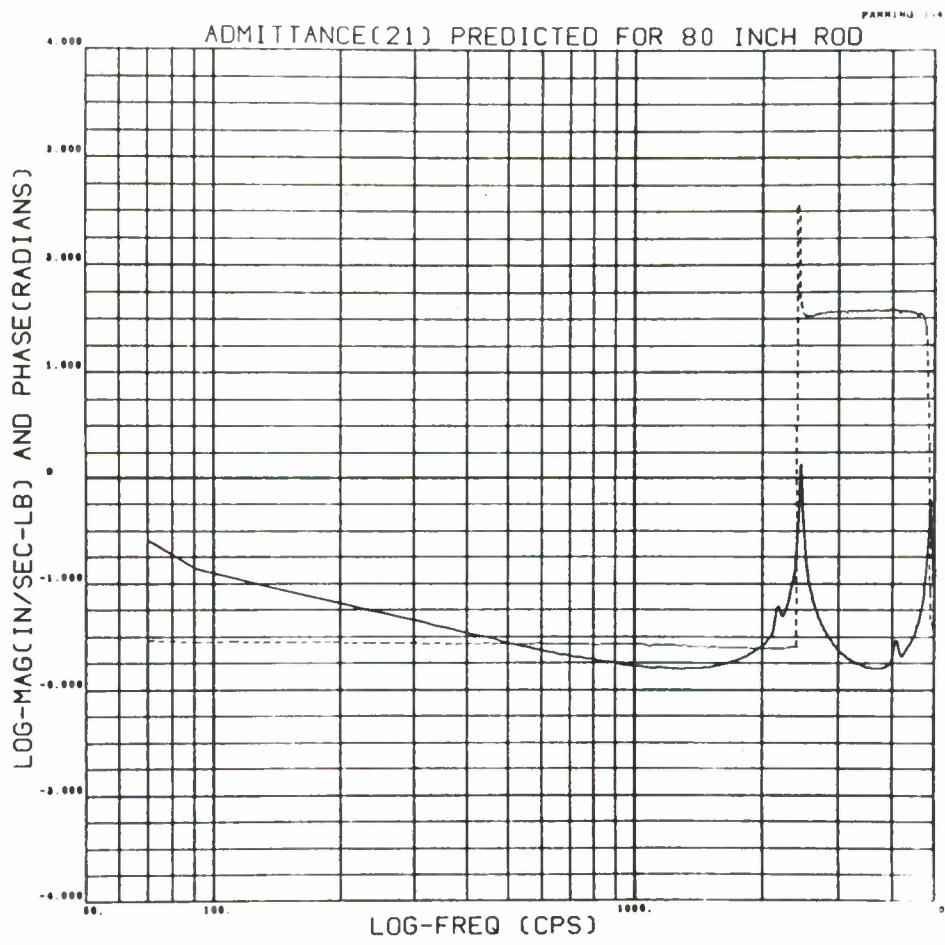


Figure 4.13

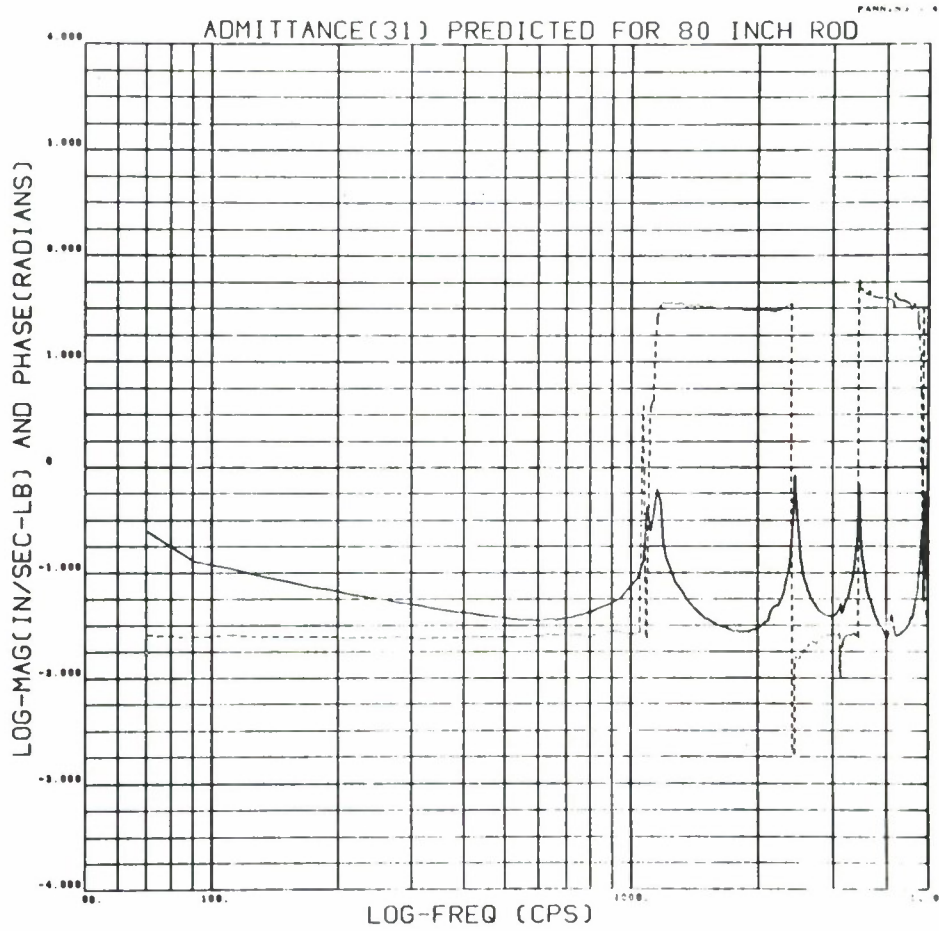


Figure 4.14

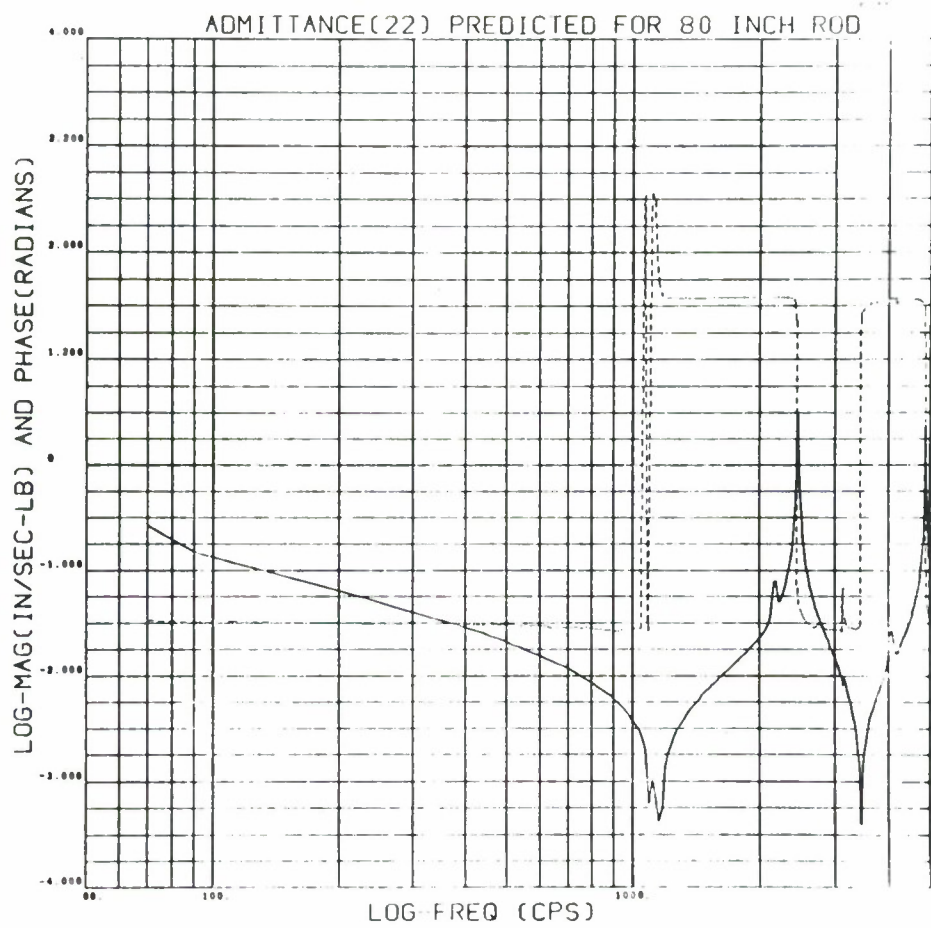


Figure 4.15

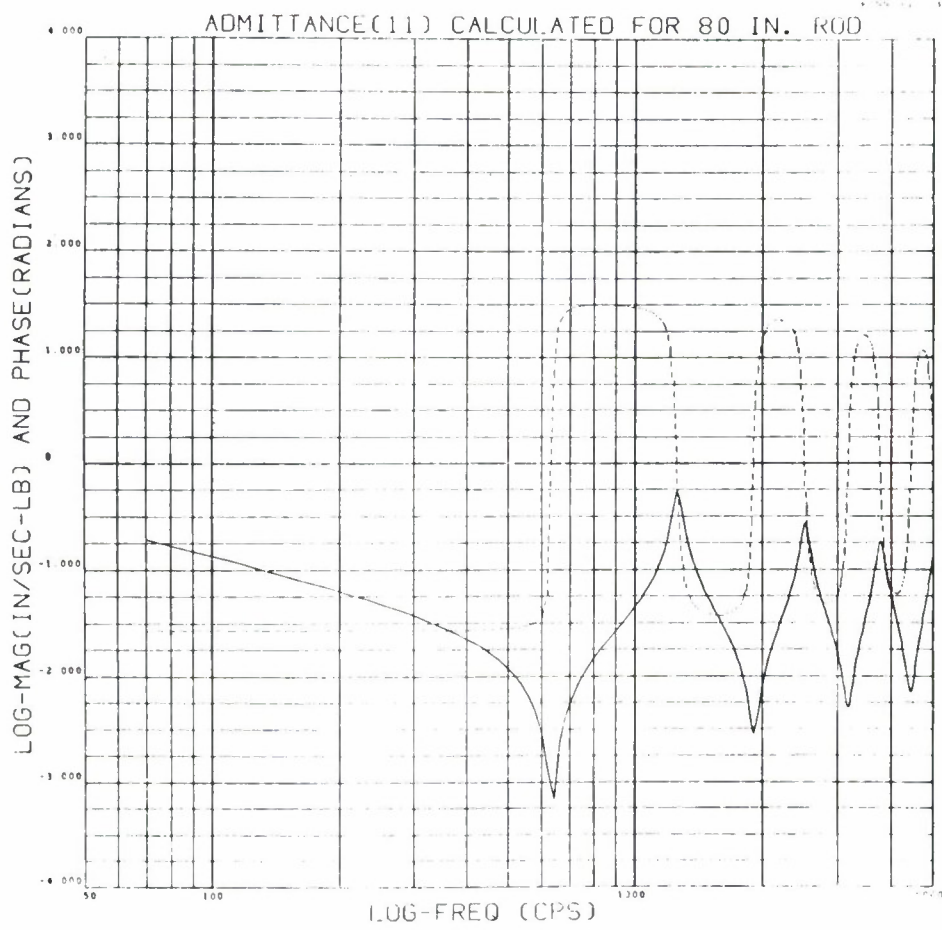


Figure 4.16

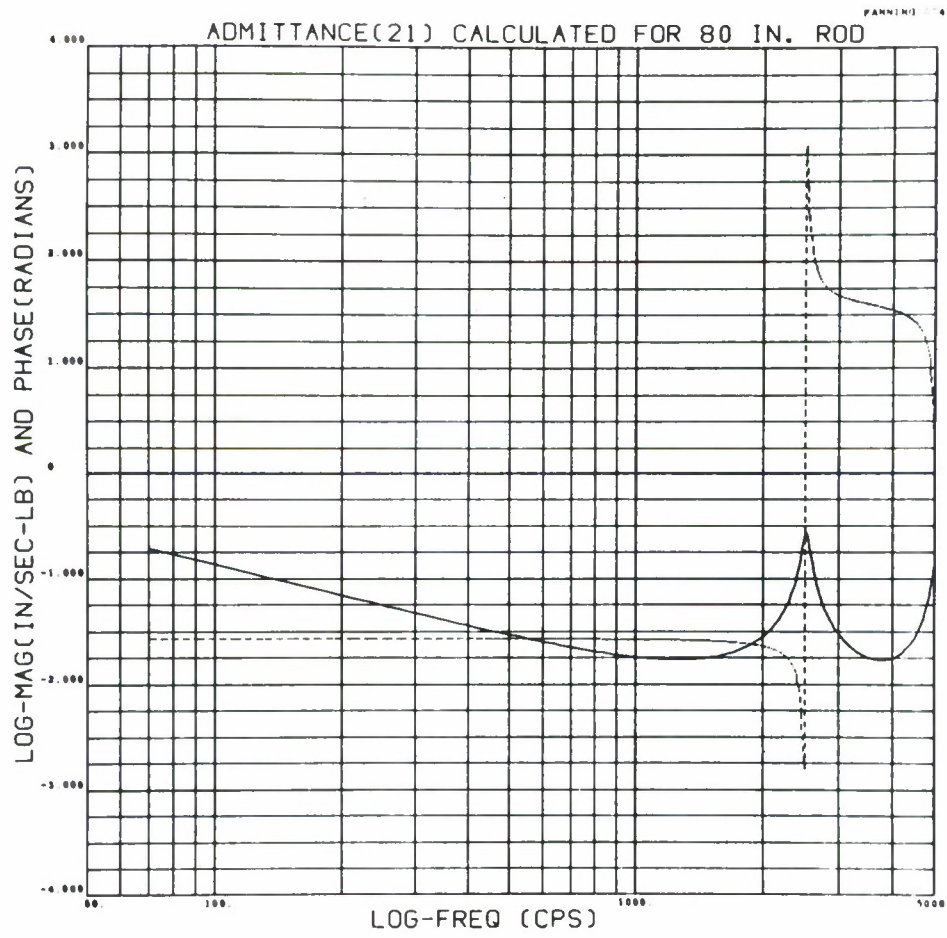


Figure 4.17

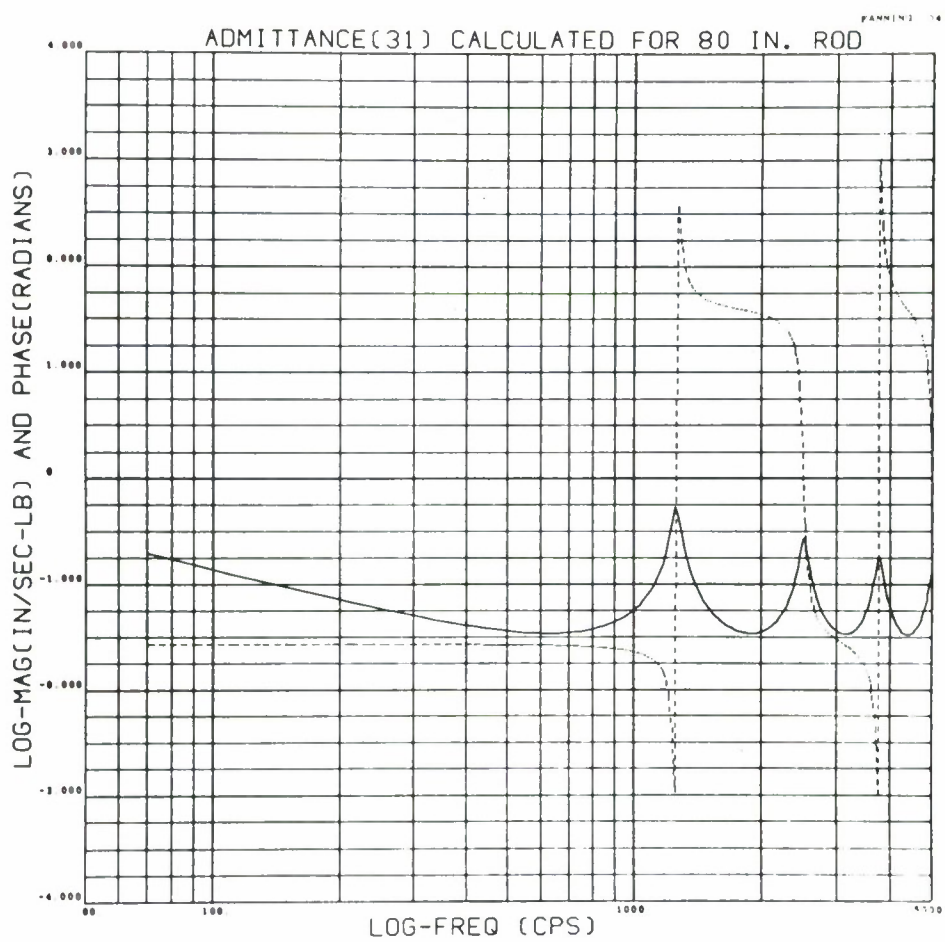


Figure 4.18

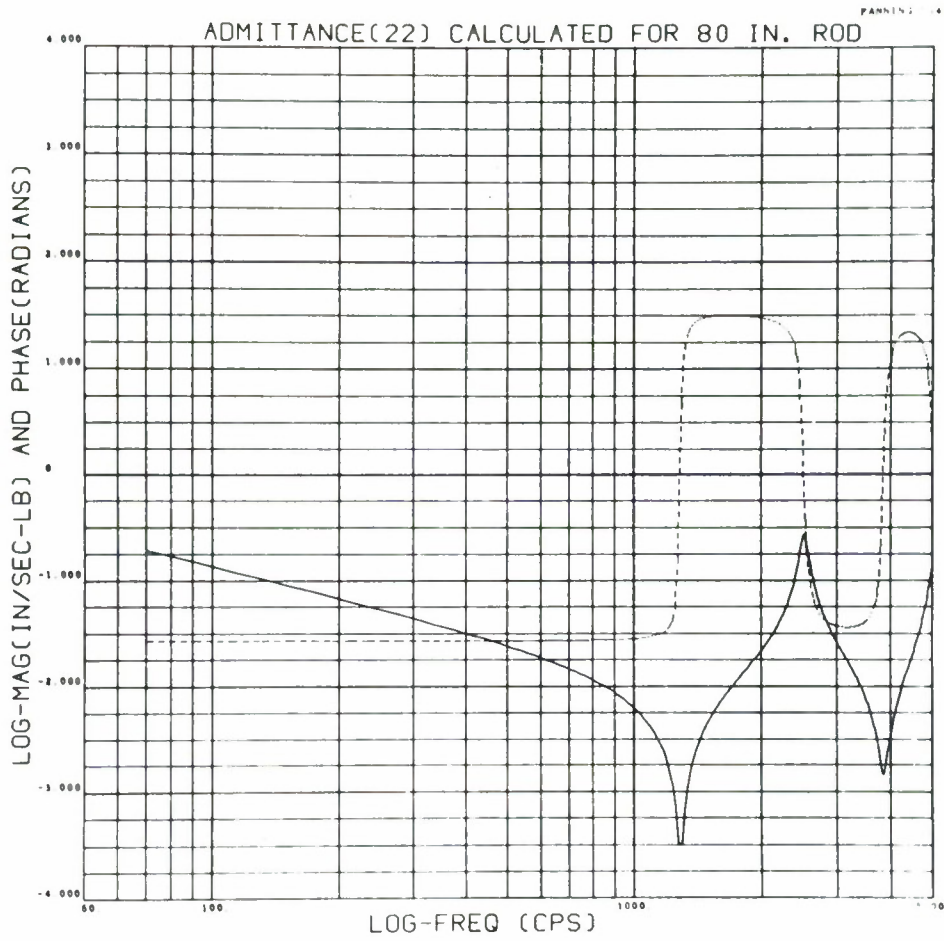


Figure 4.19

Calculated and Predicted Mode Shapes
and Resonant Frequencies

Table 4.2

| | Location | 1 | 2 | 3 | Resonant Frequency (c.p.s.) |
|---------------|------------|------|-------|--------|-----------------------------------|
| | Admittance | 11 | 21 | 31 | |
| Mode Shape | | | | | |
| 1 | Predicted | 1.0 | .053* | - .998 | 1134. |
| | Calculated | 1.0 | 0.0 | - 1.0 | 1257. |
| 2 | Predicted | 1.0 | -.238 | .142 | 2422.** |
| | Calculated | 1.0 | - 1.0 | 1.0 | 2515. |
| 3 | Predicted | .996 | .025* | - 1.0 | 3527. |
| | Calculated | 1.0 | 0.0 | - 1.0 | 3772. |
| 4 | Predicted | 1.0 | -.012 | .012 | 4815.** |
| | Calculated | 1.0 | - 1.0 | 1.0 | 5030. |

* No local maxima appear in this element of the predicted admittance matrix at or near this frequency. See section 2.4.

** These frequencies are very close to resonant frequencies of the substructures.

Equations 4.15 through 4.17 show that the measured admittances of the 40-inch rod substructure are affected by the damping of the suspension system at the first resonant frequency of the free rod. In addition equation 4.22 shows that the mass of the shaker and impedance head also distorts the admittances at the frequency ω_2^* . Consequently, the admittances predicted from admittance measurements made near the resonant frequencies of the substructures are not accurate. Therefore, if a resonant frequency of a substructure is close to a resonant frequency of the composite structure, one should not expect to predict accurately the corresponding mode shape for the composite structure.

In Table 4.2 the calculated mode shapes, $\phi^n(x)$, are defined in equation 4.26 with L equal to 80 inches. The calculated resonant frequencies are defined as follows:

$$\nu_n = \frac{\omega_n}{2\pi} = \frac{n}{2L} \left(\frac{E}{\rho} \right)^{1/2} \quad (4.31)$$

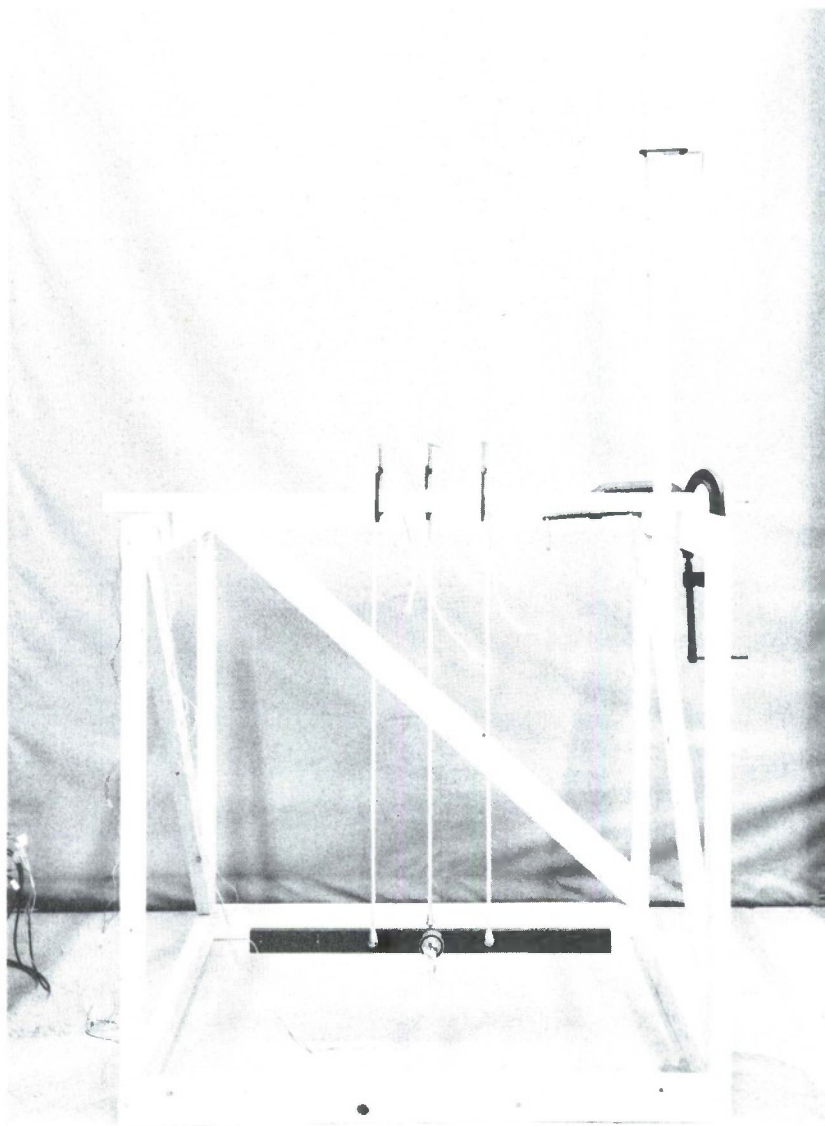
The predicted mode shapes and resonant frequencies are calculated as shown in section 2.4.

4.4 The Effects of the Suspension System on the Measured Admittances of a 32-Inch Free Beam

The Beam is suspended on three lengths of $\frac{1}{8}$ -inch shock cord to simulate a free beam. The shock cord hangs parallel to the Y axis in Figure 4.33. See also Figures 4.20 and 4.21. The beam is suspended on the shock cord such that the majority of the weight of the beam is balanced by the reaction force in the length of cord attached to the beam nearest to the point of forced excitation. Consequently, the suspension is changed every time the shaker and impedance head are attached at a new location.

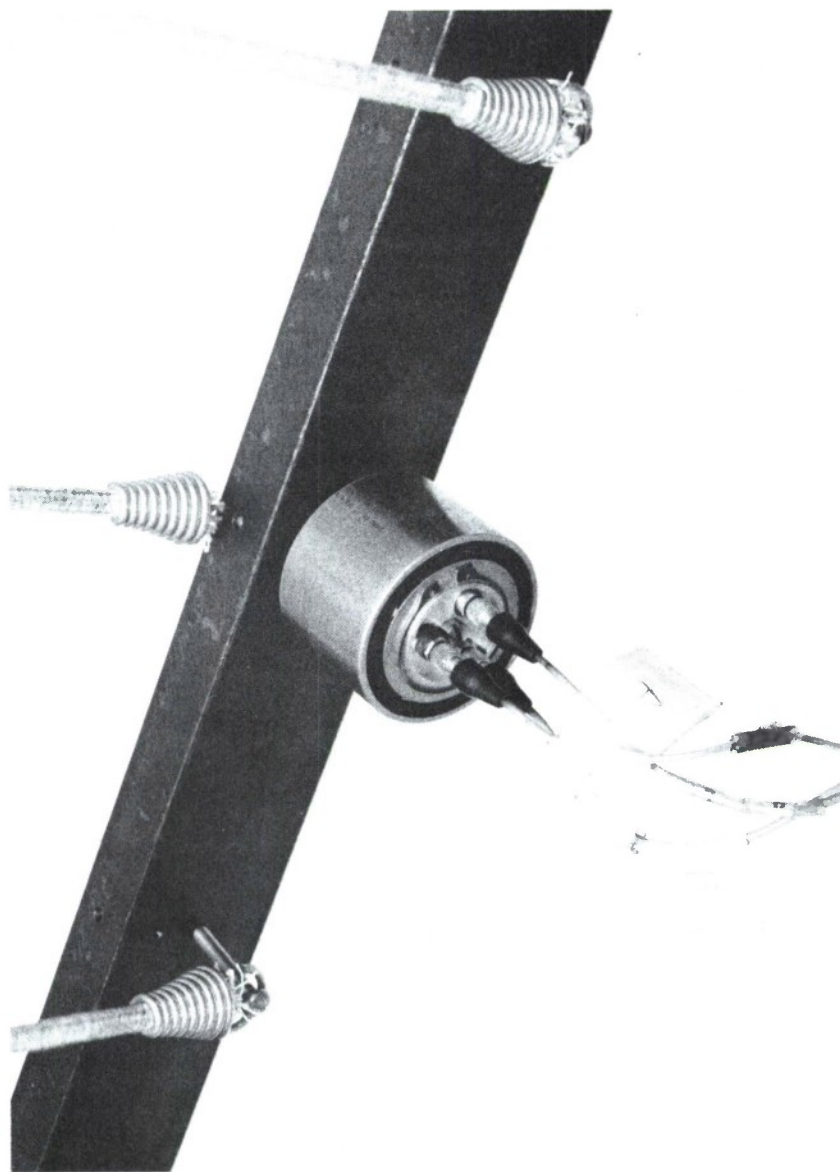
Figure 4.23 is an analog plot of the mutual admittance of location 2 on the 32-inch beam using a suspension system similar to the one shown in Figure 4.20. Figure 4.24 is an analog plot of the same admittance measured using a suspension system that supports the majority of the weight of the beam at locations not near the point of forced excitation.

Two lightweight bolts, 1.5 inches long, are put into the beam some distance away from and on both sides of the shaker and impedance head attachment point. One length of shock cord is attached to the upper flange of the beam just above the impedance head and shaker, and the other two lengths of cord are attached to the ends of the bolts. Figure 4.25 shows an X,Y plane projection of the suspension system with the shaker and impedance head attached to the beam.



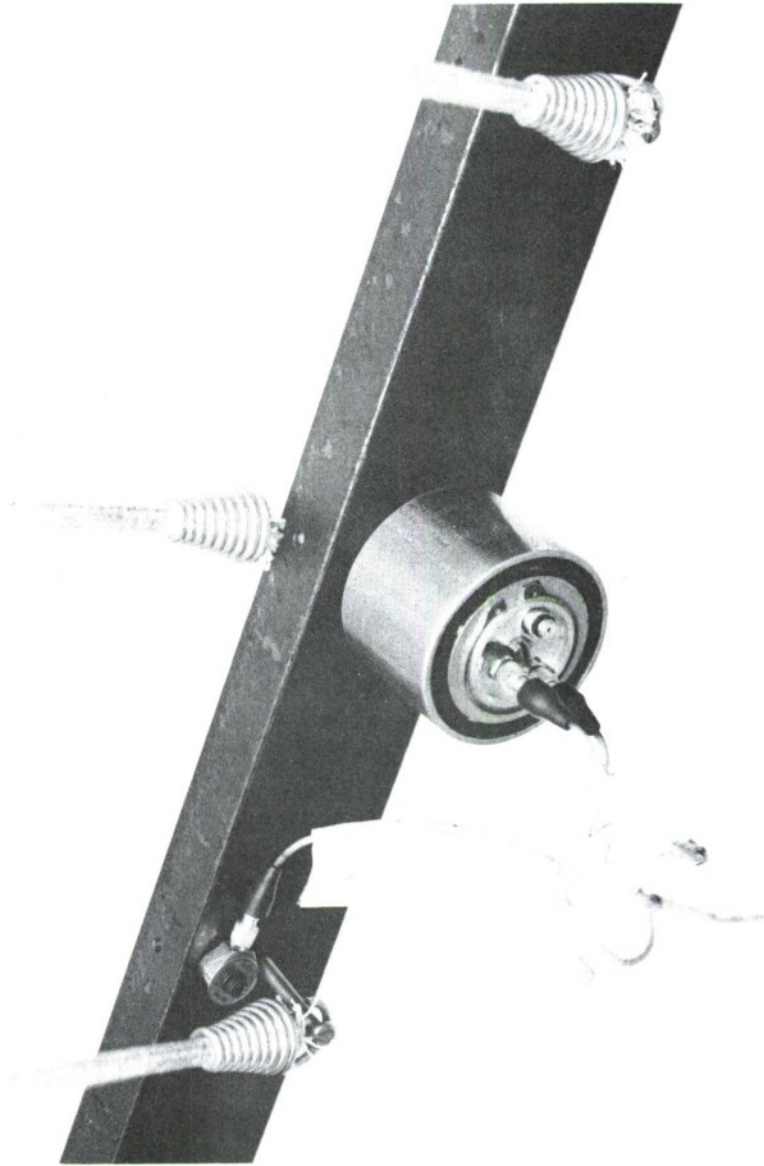
Suspension System Used to Measure the
Admittances of a 32-Inch Free Beam

Figure 4.20



Measuring a Mutual Admittance
of a 3/2-Inch Free Beam

Figure 4.21



Measuring a Cross Admittance
of a 32-Inch Free Beam

Figure 4.22

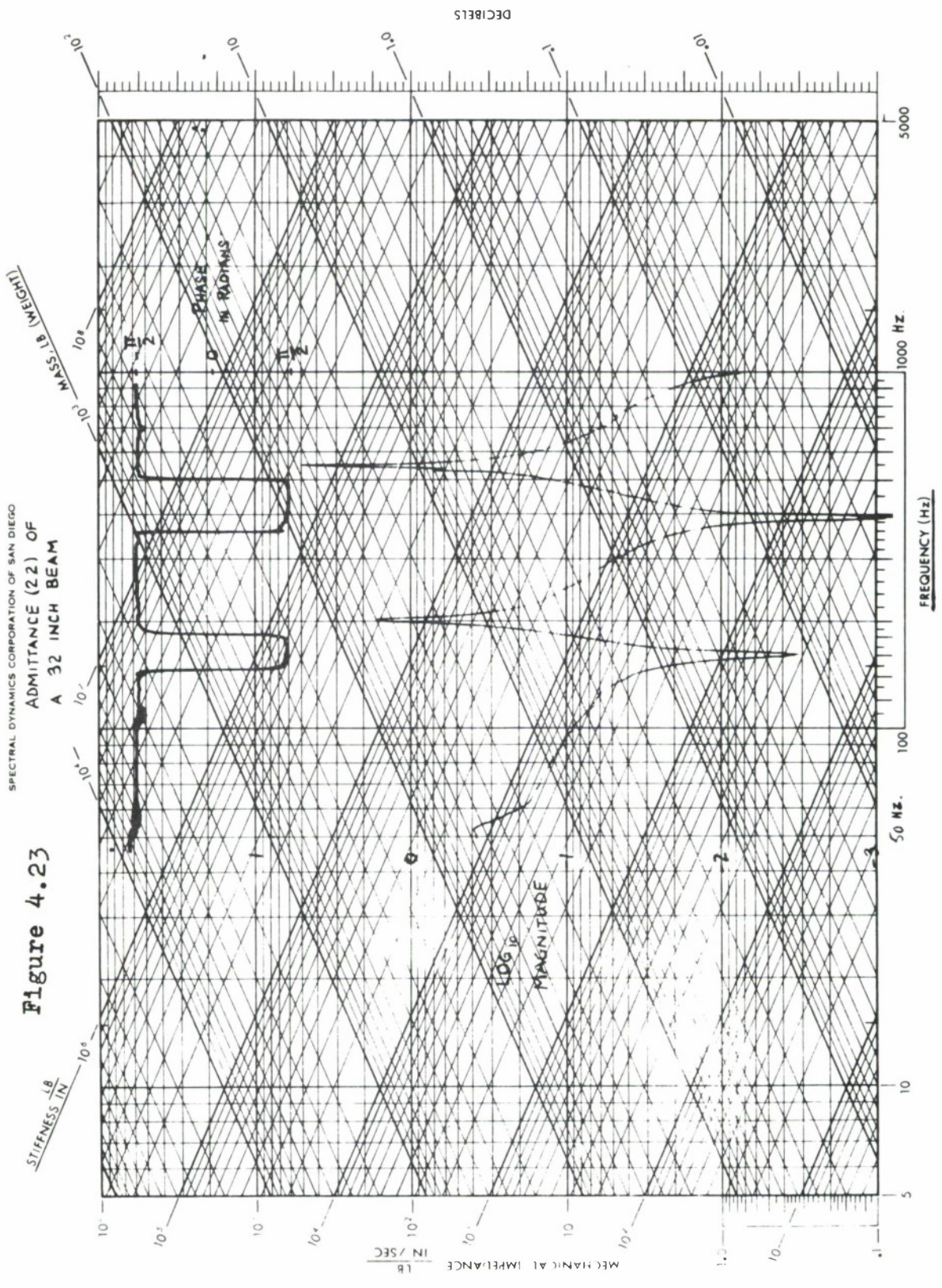
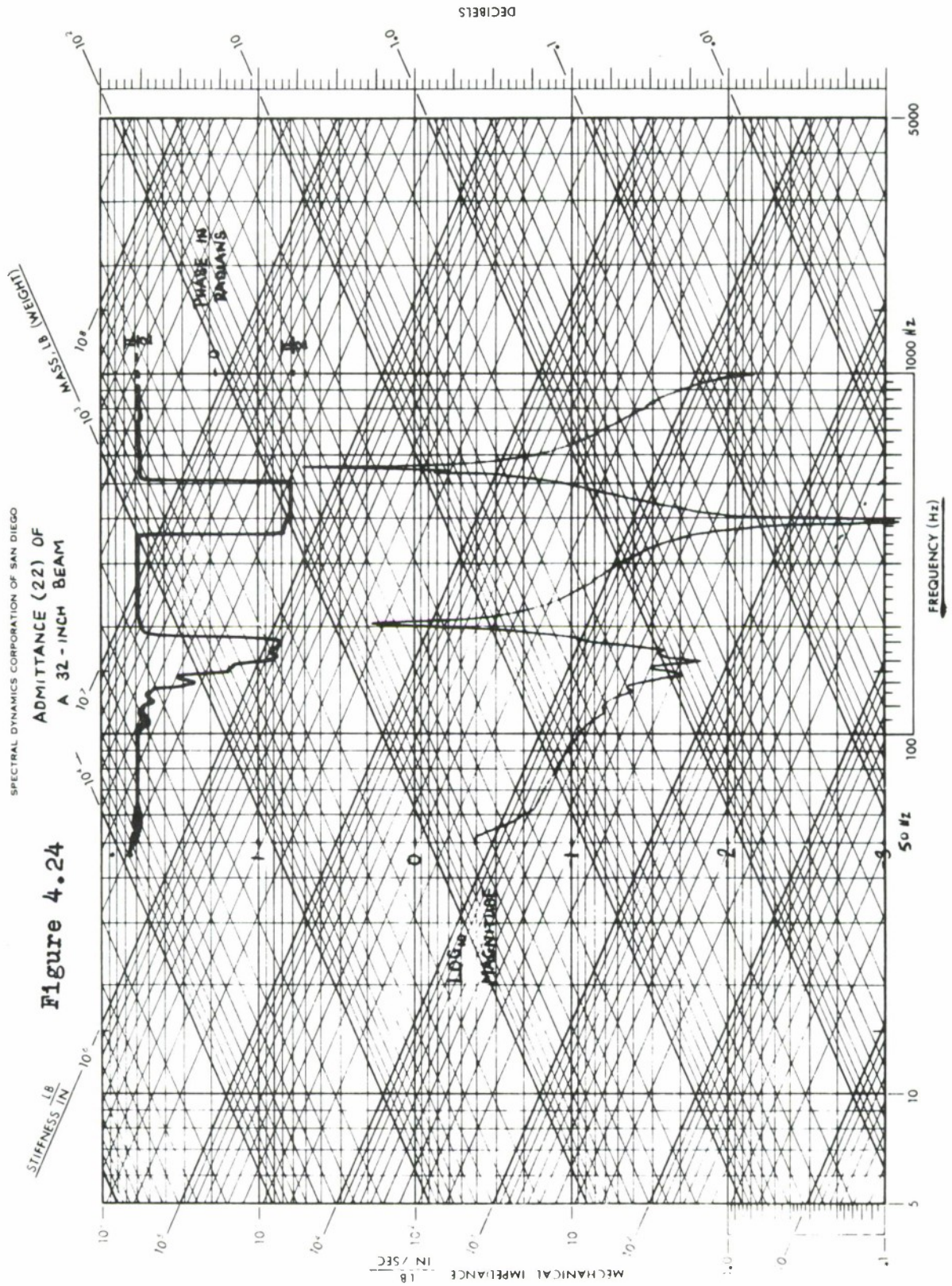
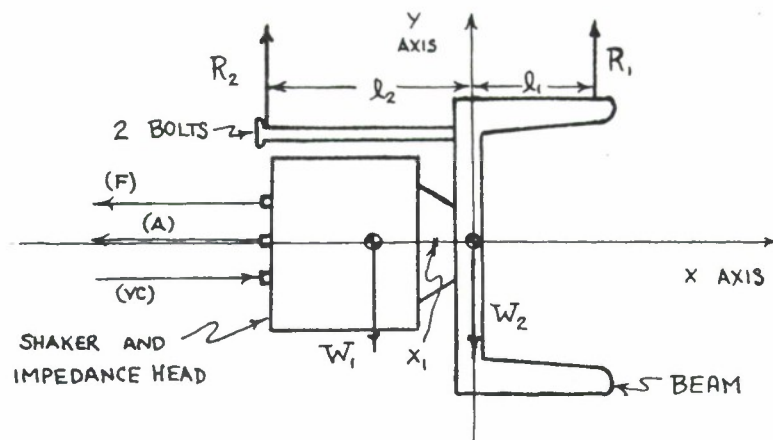


Figure 4.23

SPECTRAL DYNAMICS CORPORATION OF SAN DIEGO
ADMITTANCE (22) OF
A 32 INCH BEAM





Schematic of 32-Inch Beam Suspension System

Figure 4.25

R_1 is the deadweight reaction force in the shock cord attached to the beam near the point of forced excitation. R_2 is the sum of the deadweight reaction forces in the shock cords attached to the two bolts. W_1 and W_2 are the weights of the shaker with impedance head and the beam, respectively. The location of the center of gravity for the beam, shaker and impedance head is x_1 .

Using force equilibrium in the Y direction, equation 4.32, and moment equilibrium in the Z direction, equation 4.33, the deadweight reaction forces, R_1 and R_2 , are determined.

$$(R_2 + R_1 - W_1 - W_2) = 0. \quad (4.32)$$

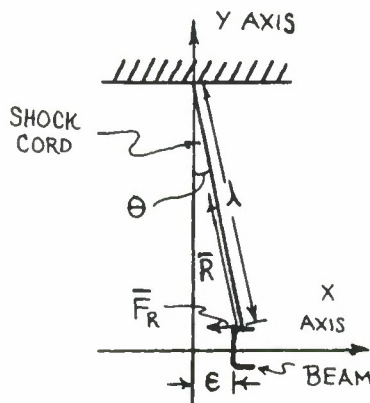
$$-R_2(l_2 + x_1) + R_1(l_1 - x_1) = 0. \quad (4.33)$$

$$R_1 = (W_1 + W_2) \frac{(l_2 + x_1)}{(l_1 + l_2)} \quad (4.34)$$

$$R_2 = (W_1 + W_2) \frac{(l_1 - x_1)}{(l_1 + l_2)} \quad (4.35)$$

Because R_2 is the sum of the two deadweight reaction forces in the shock cords attached to the bolts and each of the two deadweight reaction forces at the bolts must be positive for the suspension system to be statically stable, R_2 is the largest possible force in either of the two shock cords attached to the bolts. In general, the deadweight reaction forces in the cords attached to the bolts are different.

During the forced excitation of the beam the force in the shock cord changes very little, assuming that the motion of the shock cord is small. Assuming the angle between the shock cord and the vertical, θ , is a function of the displacement of the beam where the cord is attached, one can solve for the force exerted in the X direction by the cord on the beam, F_R .



Schematic of the Reaction Forces in the Suspension System

Figure 4.26

$$F_R = -\frac{R\epsilon}{\lambda} \quad (4.36)$$

F_R is proportional to the deadweight reaction force, R , and the local displacement of the beam, ϵ .

To simulate a free beam it is best to make the deadweight reaction forces as small as possible. The suspension system shown in Figure 4.21 is an attempt to minimize R_2 and make $R_1 \approx W_1 + W_2$. Therefore, the reaction forces, F_R , are small at locations away from the point of excitation and the reaction force at the point of excitation is, hopefully, much smaller than the force applied by the shaker.

If F_S is the force applied to the beam in the X direction by the shaker and F_{RS} is the reaction force in the X direction exerted on the beam by the shock cord attached at the point of excitation, one can solve for the measured mutual admittance.

$$Y_{\text{measured}}(\omega) = \left\{ \frac{F_S - F_{RS}}{i\omega\epsilon_s} \right\}^{-1} \quad (4.37)$$

$$F_{RS} = -\frac{R_s \epsilon_s}{\lambda} \quad (4.38)$$

ϵ_s is the local displacement of the beam at the point of excitation and R_s is the deadweight reaction force in the shock cord attached to the beam at the point of excitation.

If $R_s = W_1 + W_2$, a bound for the effect of the shock cord on the measured mutual admittance is established.

$$Y_{\text{measured}}(\omega) = \left\{ \frac{F_s}{i\omega\epsilon_s} - \frac{F_{R_s}}{i\omega\epsilon_s} \right\}^{-1} = \left\{ Y_{\text{true}}^{-1}(\omega) + \frac{W_1 + W_2}{\lambda\omega i} \right\}^{-1} = \left\{ Y_{\text{true}}^{-1}(\omega) + \frac{.226}{i\omega} \right\}^{-1} \quad (4.39)$$

For higher frequencies of excitation the effect of the dead-weight reaction force, R_s , is very small except at resonant frequencies of the beam where $Y_{\text{true}}^{-1}(\omega)$ is also very small. Consequently, the suspension system affects the admittance measurements more at or near the lower resonant frequencies of the 32-inch beam.*

The frequencies of local maxima in the measured admittances that have an accompanying phase shift of π radians are compared to calculated resonant frequencies for the 32-inch free beam.

| Resonant Frequency | Calculated ⁹ | Measured |
|--------------------|-------------------------|-------------|
| 1 | 224. c.p.s. | 206. c.p.s. |
| 2 | 628. c.p.s. | 549. c.p.s. |

Comparison of Measured and Calculated Resonant Frequencies for a 32-Inch Free Beam

Table 4.3

* See reference 8 for the calculated admittances of a free beam.

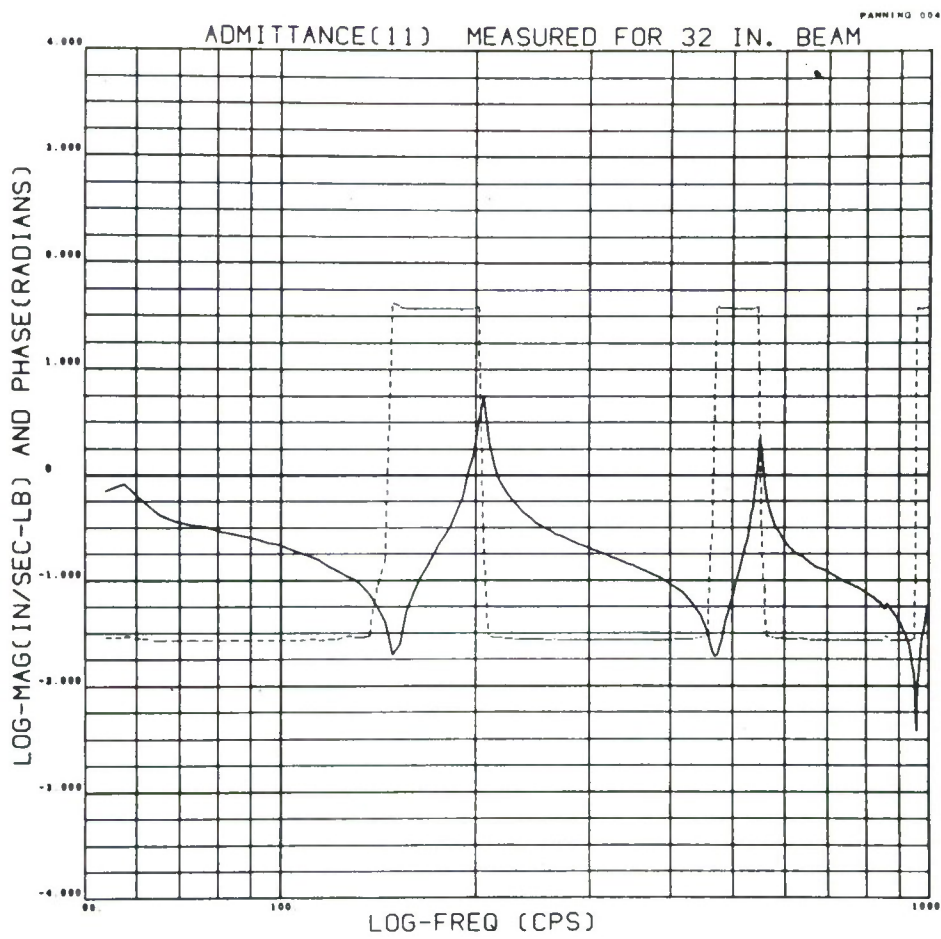


Figure 4.27

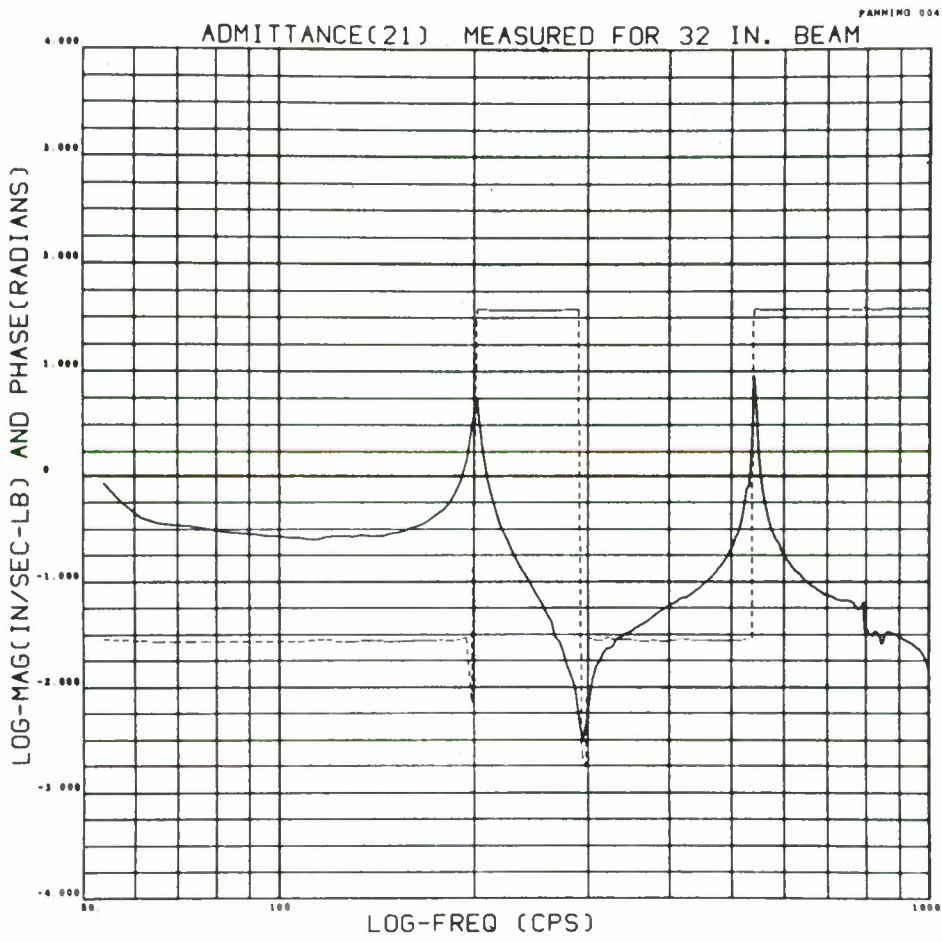


Figure 4.28

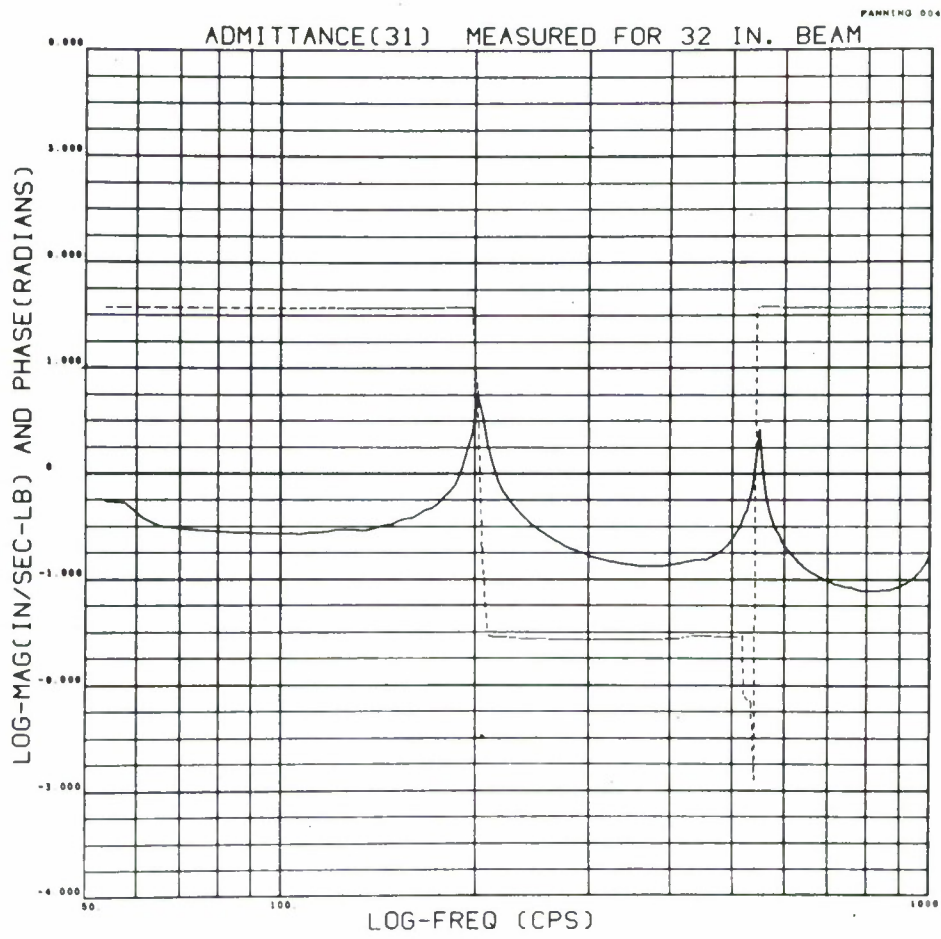


Figure 4.29

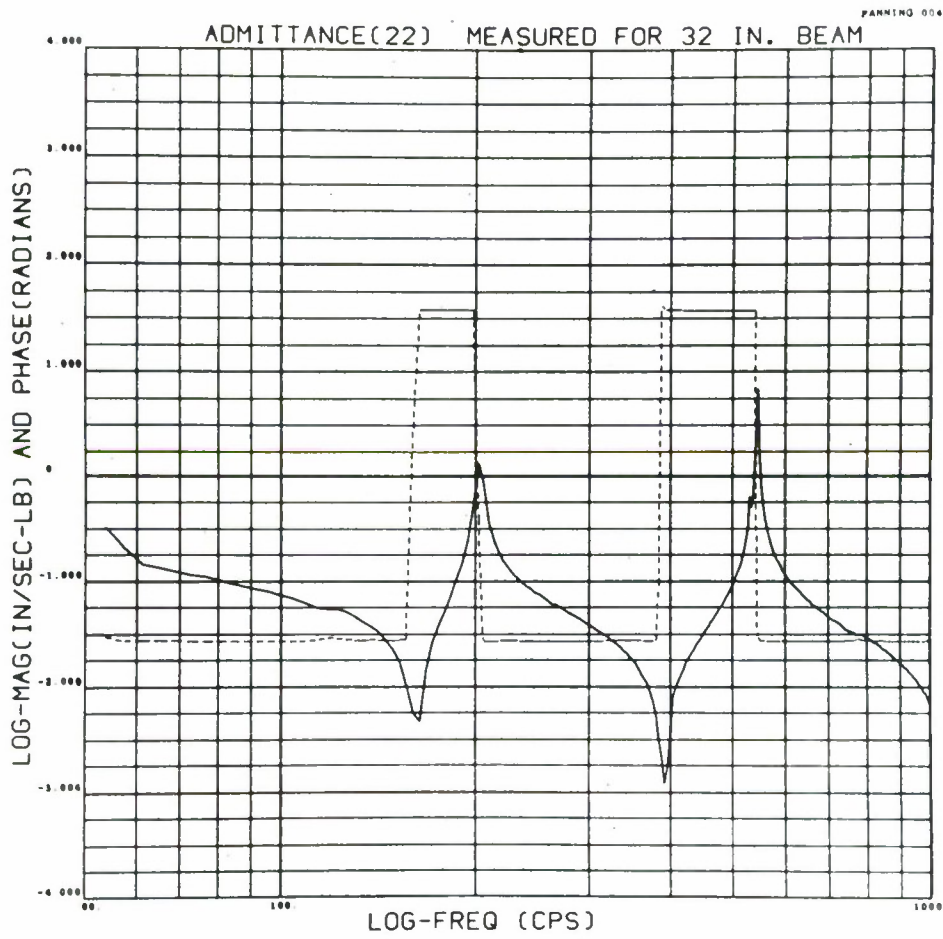


Figure 4.30

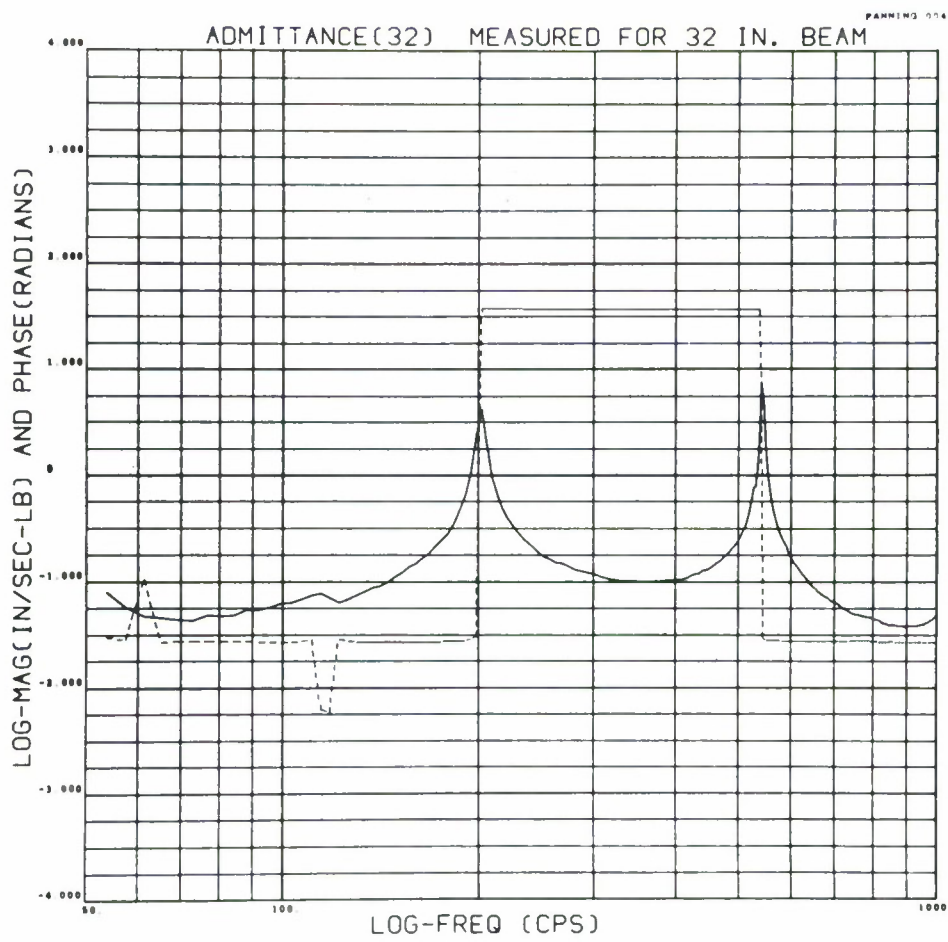
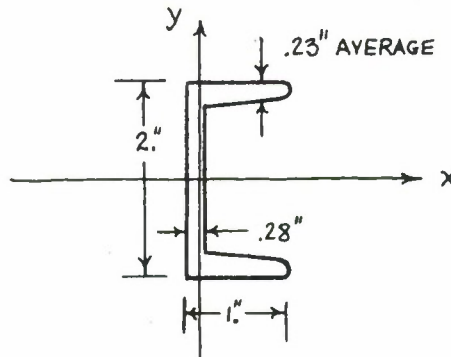


Figure 4.31

4.5 Predicting the Admittances, Resonant Frequencies and Mode Shapes for a 42-Inch Composite Beam

The admittances of a 42-inch composite beam are predicted from admittance measurements made on a 32-inch beam. The 32-inch beam has a channel cross-section and is made of steel.



Half Scale Cross Section of the Channel

Figure 4.32

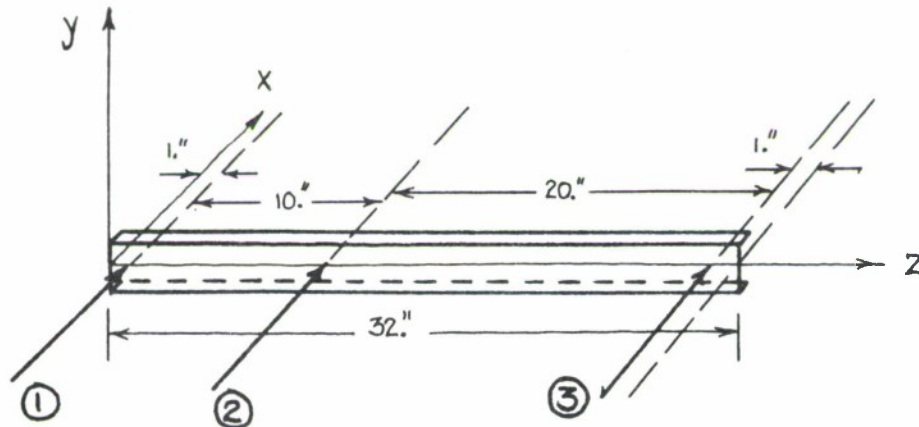
| | |
|---------------------------|--|
| I_{yy} - Moment of Area | .079 in. ⁴ |
| A - Cross-Sectional Area | .751 in. ² |
| E - Young's Modulus | 29.8×10^6 psi |
| ρ - Density | .284 $\frac{\text{lb.}}{\text{in.}^3}$ |
| L - Length | 32.0 in. |

Physical Properties of a 32-Inch Beam

Table 4.4

Admittance measurements are made at three locations on the 32-inch beam in the X direction as shown in Figure 4.33.

In general, nine admittances, three mutual admittances and six cross admittances, are needed to construct a 3×3 substructure admittance matrix. Because the admittance matrix is symmetric, one needs to measure only six admittances.



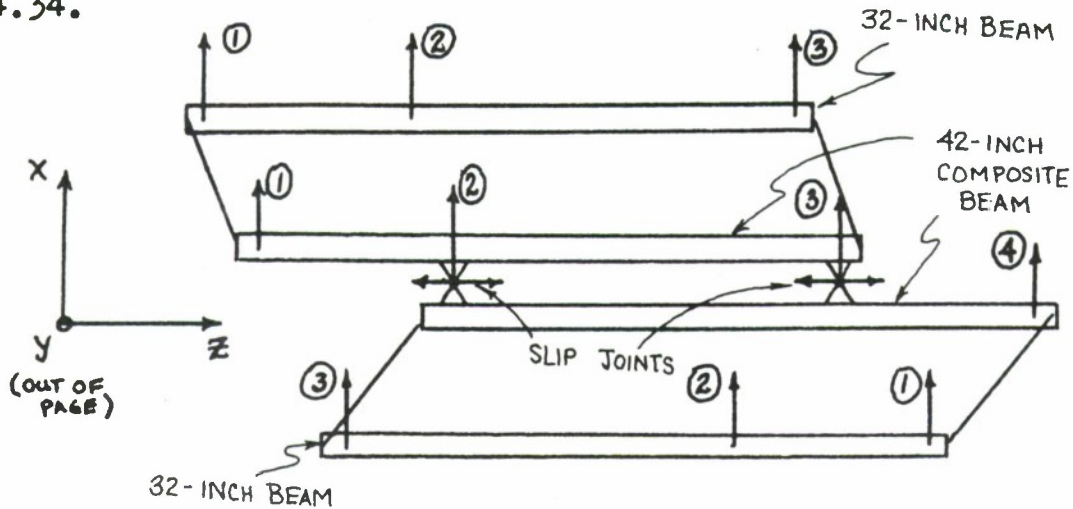
The Locations of the Measured Admittances for a 32-Inch
Beam

Figure 4.33

The mutual admittance at location 1 is the same as the mutual admittance at location 3, so the number of admittances that need to be measured is reduced to five. The five measured and sampled admittances are in Figures 4.27 through 4.31. Each admittance is sampled for 249 frequencies between 50 c.p.s. and 1000 c.p.s.

Two identical substructure admittance matrices are constructed from the measured admittances of the 32-inch beam. The substructure admittance matrices are inverted to substructure impedance matrices which are assembled into a composite structure impedance matrix as shown in section 2.2.

The composite structure is shown schematically in Figure 4.34.



Assembling a 42-Inch Composite Beam
from Two 32-Inch Free Beams

Figure 4.34

The composite structure is made of two beams pinned together at two points. At these two points of attachment the beams have compatible X displacements; however, the beams rotate independently about the Y axis at these two points. Compatibility of displacement in the Z direction at the attachment points is not necessary, since the composite structure has no degrees of freedom in the Z direction.

The composite structure impedance matrix is inverted to a composite structure admittance matrix and the mode shapes and resonant frequencies of the composite structure are estimated as shown in section 2.4. The unique elements of the composite structure admittance matrix appear in Figures 4.35 through 4.40.

The predicted resonant frequencies and mode shapes for

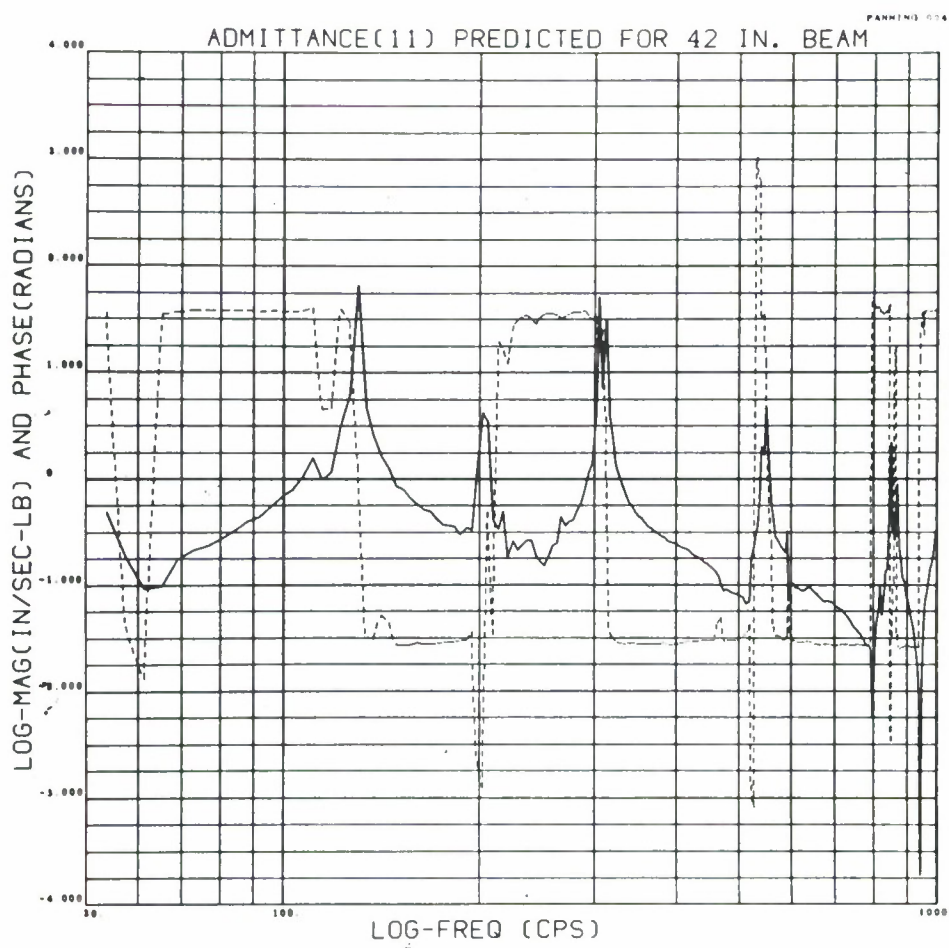


Figure 4.35

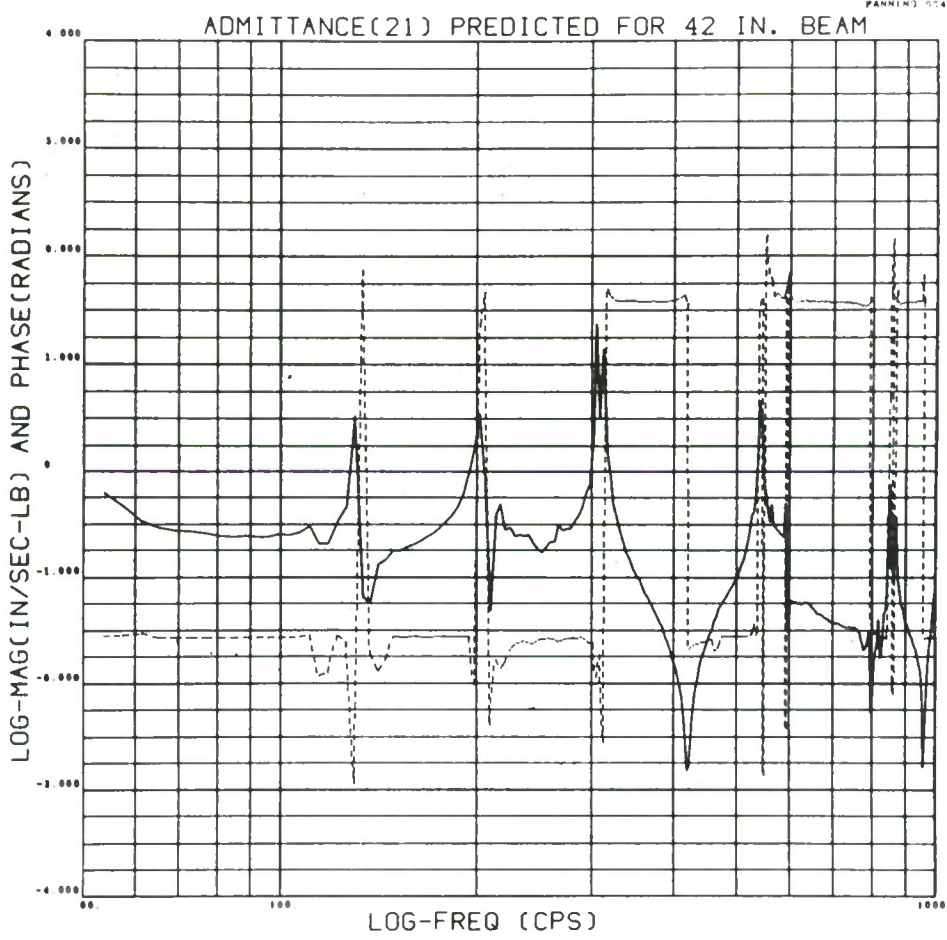


Figure 4.36

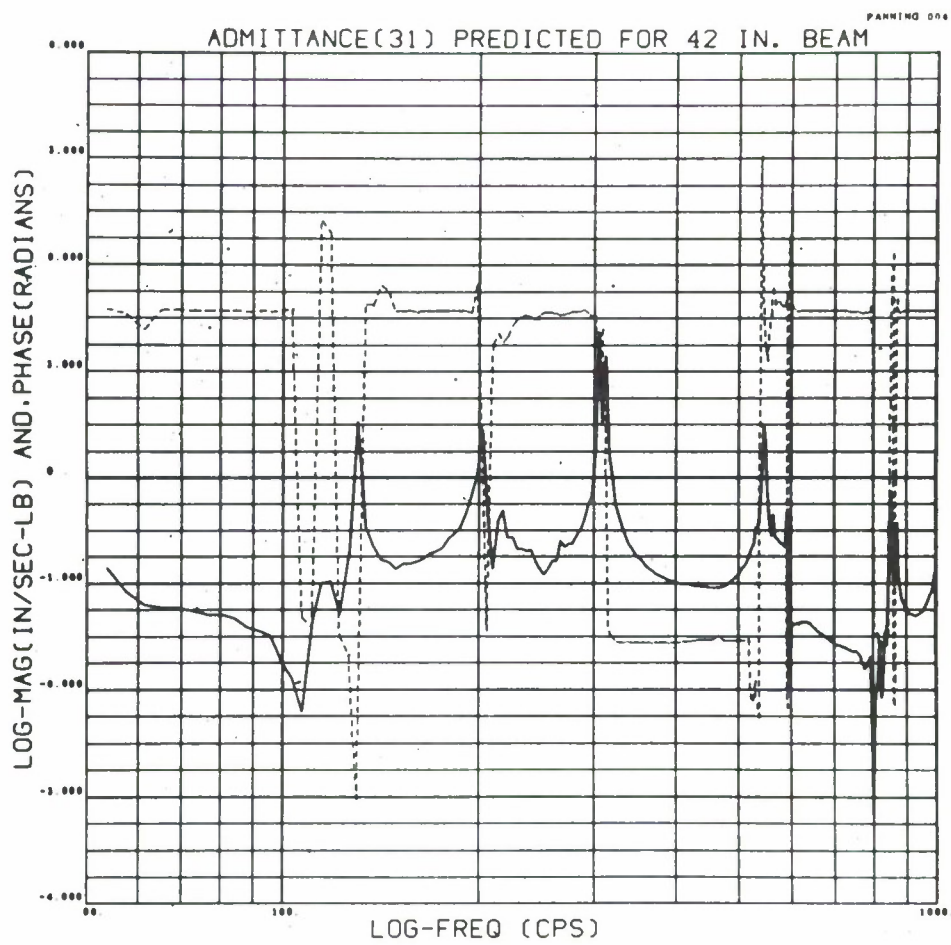


Figure 4.37

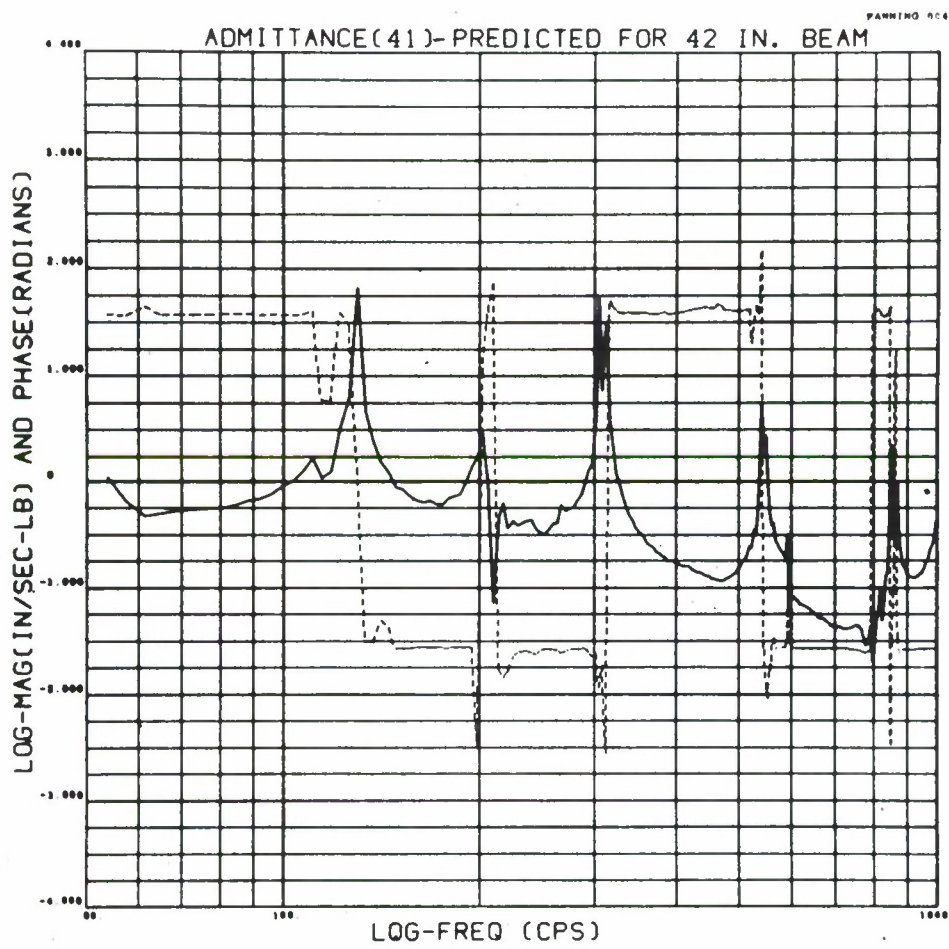


Figure 4.38

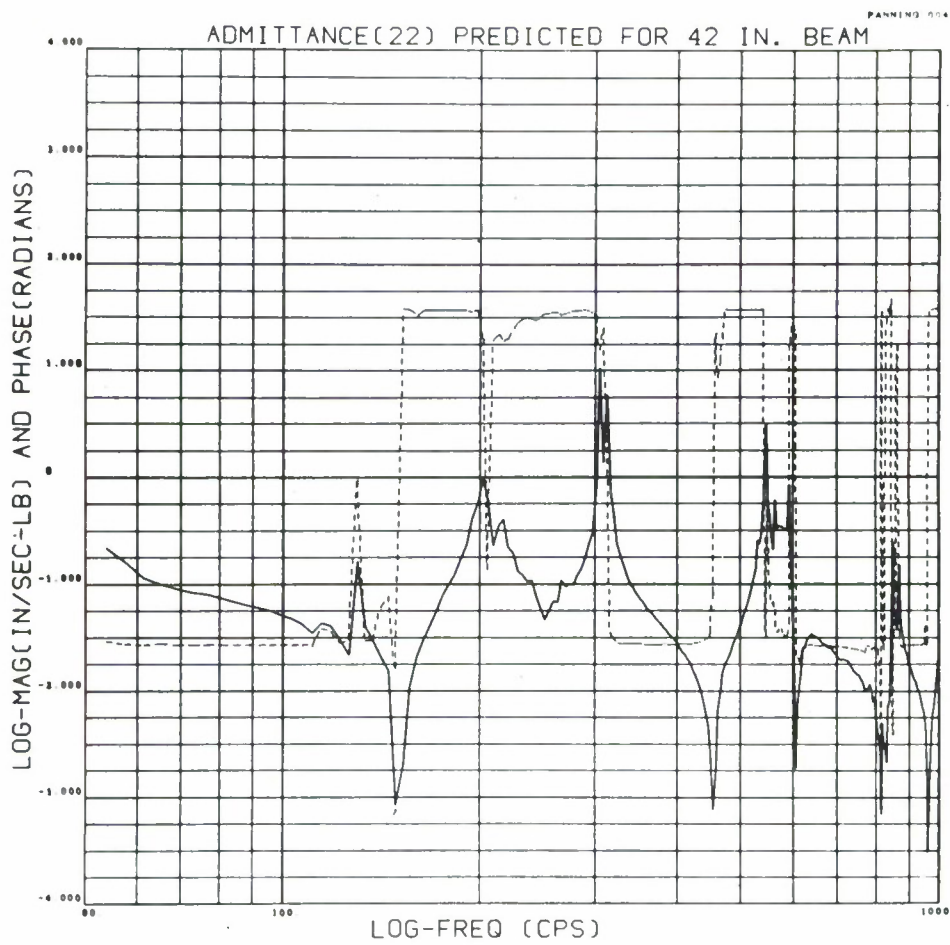


Figure 4.39

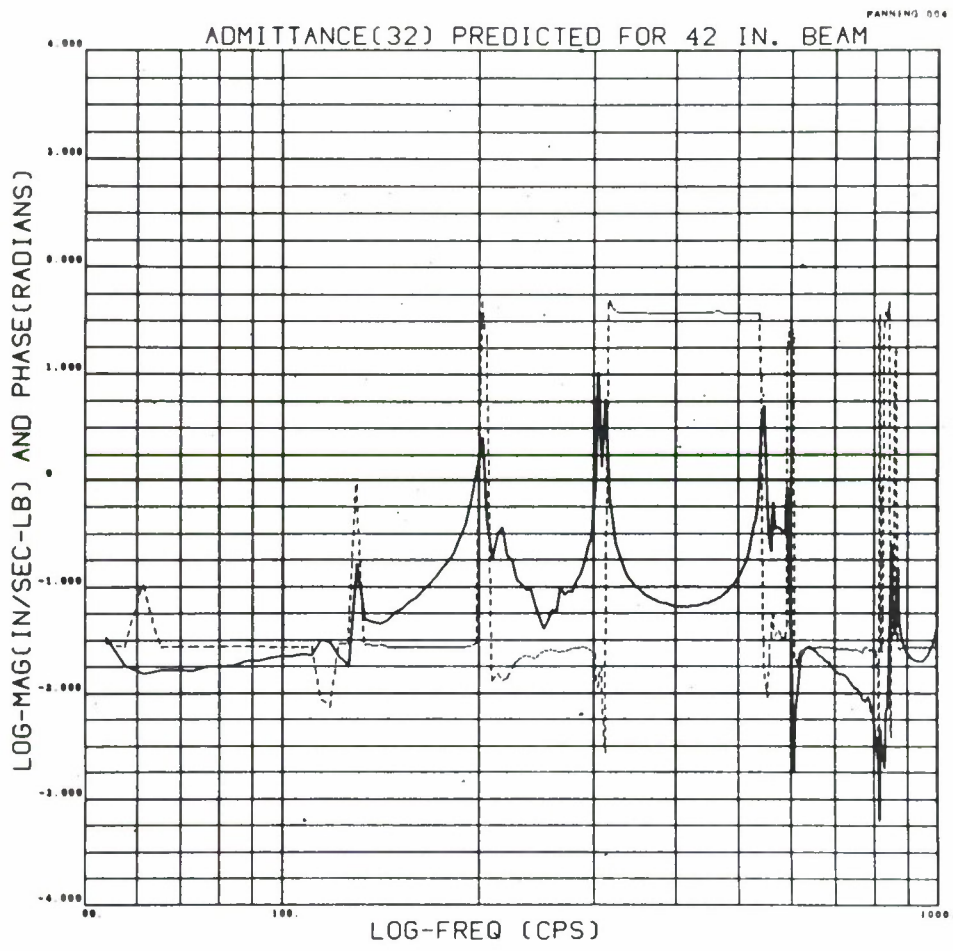


Figure 4.40

the composite structure are compared to resonant frequencies and mode shapes calculated for the composite structure.

The calculated data is generated by a finite-element computer program, STRUDL II, developed by the MIT Civil Engineering Department.^{10 11} A listing of the predicted and calculated data appears in Table 4.5.

Two of the predicted resonant frequencies of the composite structure are very close to resonant frequencies of the substructures. As shown in section 4.3 the predicted mode shapes for these two resonant frequencies of the composite structure should not be accurate due to the distortion of the measured admittances at the substructure resonant frequencies. The two resonant frequencies of the composite structure that are near resonant frequencies of the substructures correspond to the second and fourth mode shapes in Table 4.5.

Equation 4.39 shows that the effect of the suspension system on the admittance measurements should decrease with increasing frequency of excitation. If the suspension system is responsible for the inaccuracy of the second and fourth predicted mode shapes, the second mode shape should be less accurate than the fourth mode shape. The data in Table 4.5 shows that the second predicted mode shape at 202 c.p.s. is less accurate than the fourth predicted mode shape at 549 c.p.s.

The calculated resonant frequencies for the composite structure are, in general, higher than the resonant frequen-

Calculated and Predicted Mode Shapes and Resonant
Frequencies for a 42-Inch Composite Beam

Table 4.5

| Location | 1 | 2 | 3 | 4 | Resonant Frequency (c.p.s.) |
|---------------|-------|-------|-------|-------|-----------------------------------|
| Admittance* | 11 | 21 | 31 | 41 | |
| Mode Shape | | | | | |
| 1 Predicted | 1.0 | -.052 | -.052 | 1.0 | 130. |
| 1 Calculated | 1.0 | -.059 | -.059 | 1.0 | 147. |
| 2 Predicted | -1.0 | -.828 | .669 | -.715 | 202.** |
| 2 Calculated | -1.0 | .676 | -.676 | 1.0 | 205. |
| 3 Predicted | -.998 | .454 | -.453 | 1.0 | 305. |
| 3 Calculated | -1.0 | .496 | -.496 | 1.0 | 415. |
| 4 Predicted | -.893 | .839 | .578 | -1.0 | 549.** |
| 4 Calculated | -.986 | 1.0 | 1.0 | -.986 | 567. |
| 5 Predicted | .996 | -.325 | -.330 | 1.0 | 851. |
| 5 Calculated | 1.0 | .178 | .178 | 1.0 | 1022. |
| 6 Predicted | -.971 | .391 | .406 | -1.0 | 870. |
| 6 Calculated | -1.0 | .294 | -.294 | 1.0 | 1037. |

* The admittances are used only for the predicted data.

** These frequencies are near resonant frequencies of the 32-inch beam substructure.

cies predicted by the admittance data. The composite structure is modeled using the assumed displacement method which should yield calculated resonant frequencies that are upper bounds for the resonant frequencies of the real structure.

4.6 Conclusions

The resonant frequencies and mode shapes of a composite structure can be predicted using admittance measurements made on the constituent substructures if certain conditions are met. First, the shaker must be able to produce enough force to measure the admittances of the substructures over the frequency range of interest. Second, the composite must not have resonant frequencies that are very close together. Third, the suspension system must not alter the admittance measurements on the substructures. Finally, the composite structure must not have resonant frequencies that coincide with resonant frequencies of the constituent substructures.

Appendix A

The method of matrix inversion used in the computer program ADMIT is "triangular decomposition."¹² This method of matrix inversion entails decomposing a square symmetric matrix $[Y]$ into the matrix product of a matrix $[D]$ and its transpose.

$$[Y] = [D][D]^T \quad (\text{A.1})$$

The matrix $[D]$ is constructed such that all elements to the right of the principal diagonal are zero. There are the same number of unique elements in $[D]$ as there are unique elements in $[Y]$. The elements of $[D]$ are solved for using equations A.2 through A.5.

$$d_{11} = Y_{11}^{1/2} \quad (\text{A.2})$$

$$d_{n1} = Y_{n1}/d_{11} \quad (\text{A.3})$$

$$d_{nn} = \left\{ Y_{nn} - \sum_{j=1}^{n-1} d_{nj}^2 \right\}^{1/2} \quad (\text{A.4})$$

$$d_{mn} = \left\{ Y_{mn} - \sum_{j=1}^{n-1} d_{mj}d_{jn} \right\} / d_{nn} \quad m > n \quad (\text{A.5})$$

The inverse of $[Y]$ is written as a product of the inverse of $[D]$ and the transpose of the inverse of $[D]$.

$$[Y]^{-1} = [D]^{T^{-1}} [D]^{-1} \quad (\text{A.6})$$

$$[E] = [D]^{-1} \quad (\text{A.7})$$

The elements of the matrix $[E]$ are solved for using the definition of an inverse matrix, equation A.8.

$$[D][D]^{-1} = [D][E] = [I] \quad (\text{A.8})$$

Since all of the elements of $[D]$ to the right of its principal diagonal are zero, it can be shown that all of the elements of $[E]$ to the right of the principal diagonal are zero. Given all the elements of $[D]$, one can solve for the elements in $[E]$ using equations A.9 and A.10.

$$e_{nn} = d_{nn}^{-1} \quad (\text{A.9})$$

$$e_{mn} = \left\{ -\sum_{j=n}^{m-1} d_{mj}e_{jn} \right\} / d_{nn} \quad m > n \quad (\text{A.10})$$

Appendix B
Computer Program Listings

```

CP67USERID FANNING 05/04/71 15058046 FANNING *****
C AOM00010
C AOM00020
C ADMDD030
C AOM00040
C ADM00050
C AOM00060
C AOM00070
C AOM00080
C AOM00090
C AOMDD100
C AOM00110
C AOM00120
C AOM00130
C AOM00140
C AOM00150
C AOM00160
C AOM00170
C AOM00180
C AOM00190
C AOM00200
C AOM00210
C AOM00220
C AOM00230
C AOM00240
C AOM00250
C AOM00260
C AOM00270
C AOM00280
C AOM00290
C AOM00300
C AOM00310
C AOM00320
C AOM00330
C AOM00340
C AOM00350
C AOM00360
C AOM00370
C AOM00380
C AOM00390
C AOM00400
C AOM00410
C AOM00420
C AOM00430
C AOM00440
C AOM00450
C AOM00460
C AOM00470
C AOM00480
C AOM00490
C AOM00500
C AOM00510

THE COMPUTER PROGRAM ADMIT PREICTS THE ADMITTANCE MATRIX
FOR A COMPOSITE STRUCTURE FROM THE ADMITTANCE MATRICES OF THE
CONSTITUENT SUBSTRUCTURES. THE SUBSTRUCTURE ADMITTANCE MATRICES
ARE READ INTO THE MATRIX SUBAD AND ARE INVERTED TO SUBSTRUCTURE
IMPEDANCES. THE SUBSTRUCTURE IMPEDANCE MATRICES ARE ASSEMBLED
INTO A COMPOSITE STRUCTURE IMPEDANCE MATRIX AS SHOWN IN SECTION
2-2. THE COMPOSITE STRUCTURE IMPEDANCE MATRIX IS INVERTED TO
THE COMPOSITE STRUCTURE ADMITTANCE MATRIX, TOTAO. THE PREICTED
ADMITTANCE MATRICES FOR DIFFERENT FREQUENCIES OF EXCITATION ARE
STORED IN THE MATRIX OUTPUT.
ALL ADMITTANCE AND IMPEDANCE MATRICES ARE STORES IN ONE
DIMENSIONAL ARRAYS. THE ELEMENTS OF IMPEDANCE AND ADMITTANCE
MATRICES THAT ARE TO THE RIGHT OF THE PRINCIPAL DIAGONAL ARE NOT
USED BECAUSE THE MATRICES ARE SYMMETRIC. THE INTEGER FUNCTION
TOENT IS USED TO ADDRESS THE ELEMENTS OF THE SQUARE IMPEDANCE
AND ADMITTANCE MATRICES IN ONE DIMENSIONAL ARRAYS.

SM IS THE NUMBER OF SUBSTRUCTURE ADMITTANCE MATRICES USED TO
CALCULATE THE COMPOSITE STRUCTURE ADMITTANCE MATRIX.

OSM IS THE DIMENSION OF THE LARGEST SUBSTRUCTURE ADMITTANCE
MATRIX

OTM IS THE DIMENSION OF THE COMPOSITE STRUCTURE ADMITTANCE
MATRIX

OP IS THE NUMBER OF FREQUENCIES FOR WHICH SUBSTRUCTURE ADMIT-
TANCE MATRICES HAVE BEEN CONSTRUCTED.

FBL AND FBU ARE THE LOWER AND UPPER BCUNDS FOR THE FREQUENCY
SWEEP THAT GENFRATED THE ADMITTANCE DATA.

IDIS IS THE MATRIX THAT CONTAINS THE NODE NUMBERS FOR THE
COMPOSITE STRUCTURE FOR EACH OF THE NOCES ON THE CONSTITUENT
SUBSTRUCTURES.

DIMENSION SUBAD(6),TOTAO(110),IDIS(3,3),OATAI249,2,6,2)
DIMENSION OUTPUT2,10,249)
COMPLEX SUBAD,TOTAO,TOTA,CTOTAD,STORE,CTCKE
10 FORMAT(20,1C)
20 FORMAT(4E19,1D)
1001 FORMAT(1D,0)
1005 FORMAT(1F8,2)
1002 FORMAT(2I20,10,5X)
1000 FORMAT(1911)
C

```



```

C          STRUCTURE IMPEDANCE MATRICES.
C
C          DD 205 N=I, ICSN
C          NI=N-1
C          IF(NI.EQ.0) GO TO 204
C          DD 202 I=1, NI
C          II=I-1
C          STDRF=(0.,0.)
C          IF(I.EQ.1) GO TO 201
C          DD 200 M=1, II
C          STORE=STORE+SUPAD(IDENT(N,M))*SUBAD(IDENT(I,M))
C          200 CONTINUE
C          201 SUBAD(IDENT(N,I))=(SUBAD(IDENT(N,I))-STORE)/SUBAD(IDENT(I,I))
C          202 CONTINUE
C          STDRF=(0.,0.)
C          DD 203 M=1, NI
C          STORE=STORE+SURAD(IDENT(N,M))*Z
C          203 CONTINUE
C          204 IF(NI.EQ.0) STORE=(0.,0.)
C          SUBAD(IDENT(N,N))=CSORT(SUBAD(IDENT(N,N))-STORE)
C          205 CONTINUE
C          DD 207 N=1, ICSN
C          NI=N-1
C          IF(NI.EQ.0) GO TO 210
C          DD 208 I=1, NI
C          II=I-1
C          STORE=(0.,0.)
C          DD 209 M=1, NI
C          STORE=STORE-SUPAD(IDENT(I,M))*SUBAD(IDENT(N,M))
C          209 CONTINUE
C          SUBAD(IDENT(N,I))=STORE/SUBAD(IDENT(N,N))
C          208 CONTINUE
C          210 SUBAD(IDENT(N,N))=(1.,0.) / SUBAD(IDENT(N,N))
C          207 CONTINUE
C          DD 211 N=1, ICSN
C          NI=N-1
C          DD 212 I=1, N
C          STORE=(0.,0.)
C          DD 213 M=N, ICSN
C          STORE=STORE+SUPAD(IDENT(M,N))*SUBAD(IDENT(M,I))
C          213 CONTINUE
C          SUBAD(IDENT(N,I))=STORE
C          212 CONTINUE
C          211 CONTINUE
C
C          THE SUBSTRUCTURE IMPEDANCES ARE ASSEMBLED INTO A COMPOSITE
C          STRUCTURE IMPEDANCE MATRIX.
C
ADM01060
ADM01070
ADM01080
ADM01090
ADM01100
ADM01110
ADM01120
ADM01130
ADM01140
ADM01150
ADM01160
ADM01170
ADM01180
ADM01190
ADM01200
ADM01210
ADM01220
ADM01230
ADM01240
ADM01250
ADM01260
ADM01270
ADM01280
ADM01290
ADM01300
ADM01310
ADM01320
ADM01330
ADM01340
ADM01350
ADM01360
ADM01370
ADM01380
ADM01390
ADM01400
ADM01410
ADM01420
ADM01430
ADM01440
ADM01450
ADM01460
ADM01470
ADM01480
ADM01490
ADM01500
ADM01510
ADM01520
ADM01530
ADM01540
ADM01550
ADM01560
ADM01570

```



```

CP67USERIO FANNING 05/04/71 15058049 FANNING *****
C CON0010
C CON0020
C CON0030
C CON0040
C CON0050
C CON0060
C CON0070
C CON0080
C CON0090
C CON0100
C CON0110
C CON0120
C CON0130
C CON0140
C CON0150
C CON0160
C CON0170
C CON0180
C CON0190
C CON0200
C CON0210
C CON0220
C CON0230
C CON0240
C CON0250
C CON0260
C CON0270
C CON0280
C CON0290
C CON0300
C CON0310
C CON0320
C CON0330
C CON0340
C CON0350
C CON0360
C CON0370
C CON0380
C CON0390
C CON0400
C CON0410
C CON0420
C CON0430
C CON0440
C CON0450
C CON0460
C CON0470
C CON0480
C CON0490
C CON0500

THE COMPUTER PROGRAM CONVERT INCORPORATES THE SUBROUTINE
RADATA TC CONVERT THE FORMAT OF THE DATA FROM THE RAC(ATION
A/O CONVERTER TO A FORMAT COMPATIBLE WITH THE IBM 360 COMPUTER.
THE PROGRAM CONVERTS THE FORMAT OF THE DATA ONE FILE AT A TIME.

CALL TAPSET(1,11,4096,3,1,4096)
DIMENSION STOR(2048)
FORMAT(' PARITY ERROR,M=',I4)
FORMAT(E20.10)
00 9 N=1,2048
STORE(N)=0.
CONTINUE
MFILE=1
NREC=249
00 7 N=1,NFILE
00 1 M=1,NREC
CALL RADATA(1,STORE,NC)
GO TO (4,2,7),NC
WRITE(2,3) M
STOR=0.
00 5 I=1848,2048
STOR=STOR+STOR(I)
CONTINUE
STOR=STOR/200.
WRITE(12,8) STOR
CONTINUE
CONTINUE
END

FORN1 JANUARY 1970 SUBROUTINE RADATA(NSKP,ARRAY,NCODE)
READ, CONVERT DATA ON TAPE GENERATED BY A TC C CONVERTER
SUBROUTINE RADATA(NSKP,ARRAY,NCODE)
READ ONE RECORD OF 4096 CHARACTERS AND CONVERT DATA OR
SKIP TO THE END OF FILE MARK NC DATA
CONVERSION OF DATA IS TWO SIX BIT BINARY INTEGERS COMBINED
INTO ONE BINARY INTEGER. THE FIRST SIX BIT INTEGER READ IS
THE HIGH ORDER BITS. THE INTEGER (S THEN CONVERTED TO A
FLOATING POINT NUMBER.
NSKP= 1 SAME FILE READ AND CONVERT DATA
NSKP= 2 NEXT FILE SKIP TO NEXT FILE. 00 NOT CONVERT DATA
ARRAY= DATA ARRAY
ASSUMES REAL*4 ARRAY(2048)
NCODE= 1 DATA OK CONVERT
NCODE= 2 PARITY ERROR DETECTED HOWEVER CONVERT DATA

```



```
C      BACKSPACE IUNIT
400  NCCE = 3
      IFILE= IFILE + 1
      WRITE (6,410) IREC,IFILE
410  FORMAT(' END OF FILE DETECTED AFTER RECORD',I5,' FOR FILE',I3)
      IREC= C
500  RETURN
      ENO
```

```
CON01050
CON01060
CON01070
CON01080
CON01090
CON01100
CON01110
CON01120
```

```

CP67USERIC FANNING 05/04/71 15058051 FANNING *****
C SCA00010
C SCA00020
C SCA00030
C SCA00040
C SCA00050
C SCA00060
C SCA00070
C SCA00080
C SCA00090
C SCA00100
C SCA00110
C SCA00120
C SCA00130
C SCA00140
C SCA00150
C SCA00160
C SCA00170
C SCA00180
C SCA00190
C SCA00200
C SCA00210
C SCA00220
C SCA00230
C SCA00240
C SCA00250
C SCA00260
C SCA00270
C SCA00280
C SCA00290
C SCA00300
C SCA00310
C SCA00320
C SCA00330
C SCA00340
C SCA00350
C SCA00360
C SCA00370
C SCA00380
C SCA00390
C SCA00400
C SCA00410
C SCA00420
C SCA00430
C SCA00440
C SCA00450
C SCA00460
C SCA00470
C SCA00480
C SCA00490
C SCA00500

THE PROGRAM SCALE IS INTENDE TO BE USED ON A TIME
SHARING SYSTEM TO SCALE THE CONVERTED DIGITAL DATA FROM
THE RADIATION A/D CONVERTER. THE METHOD OF SCALING IS
EXPLAINED IN CHAPTER 3 OF THIS PAPER.

THE PROCEDURE FOR USING THE PROGRAM IS AS FOLLOWS.

1. FROM THE CONSOLE PUT IN THE VALUES OF THE LOWER AND UPPER
BOUNDS OF THE FREQUENCY SWEEP AS WELL AS THE NUMBER OF DATA
POINTS FOR WHICH THE DATA IS SAMPLED.

2. ENTER THE SUBSCRIPTS OF THE FREQUENCIES FOR WHICH THE DATA
HAS BEEN SAMPLED.

3. THE FREQUENCIES THAT HAVE BEEN CHOSEN WILL BE TYPED AT THE
CONSOLE.

4. IF YOU DO NOT WANT TO USE DATA CORRESPONDING TO THESE TWO
FREQUENCIES TO SCALE ALL THE DATA TYPE IN A 0 , AND REPEAT
STEPS 2 AND 3.

5. IF THE FREQUENCIES ARE ACCEPTABLE THEN TYPE A 1 FOR A
MAGNITUDE SCALING OR A 2 FOR A PHASE SCALING.

TYPE IN THE VALUES OF THE MAGNITUDE OR PHASE FROM THE
ANALOG PLOT FOR THE TWO FREQUENCIES AND THE ENTIRE SET OF DATA
IS SCALED AS SHOWN IN CHAPTER 3.

FBI AND FB2 ARE THE LOWER AND UPPER BOUNDS OF THE FREQUENCY
SWEEP THAT GENERATED THE AMPLITUDE DATA.

OP IS THE NUMBER OF DATA POINTS IN THE ENTIRE DATA SET.

SP1 AND SP2 ARE THE SUBSCRIPTS OF THE FREQUENCIES FOR WHICH
DIGITAL DATA IS COMPARED TO PLOT DATA.

RMAG1 AND RMAG2 ARE THE VALUES OF PLOT DATA READ IN FROM THE
CONSOLE.

DIMENSION DATA(249)
READ(5,100)FBI,FB2,CP
100 FORMAT(10.0)
10P=OP

```

```

SCA00510
SCA00520
SCA00530
SCA00540
SCA00550
SCA00560
SCA00570
SCA00580
SCA00590
SCA00600
SCA00610
SCA00620
SCA00630
SCA00640
SCA00650
SCA00660
SCA00670
SCA00680
SCA00690
SCA00700
SCA00710
SCA00720
SCA00730
SCA00740
SCA00750
SCA00760
SCA00770
SCA00780
SCA00790
SCA00800
SCA00810
SCA00820

102 READ(I1,I06)(DATA(M),M=1,ICP)
   FORMAT(E20.10)
1 READ(5,100)SPI,SP2
   SPI=SPI
   ISP2=SP2
   FQ1=(F8U-FBL)/FP
   FQ1=FQ1*SPI+F8L
   FQ2=FQ1*SP2+F8L
   WRITE(6,103) FQ1,FQ2
103 FORMAT(I2(F8.2,5X))
   READ(5,104) ICHECK
104 FORMAT(I1)
   IF(ICHECK.EQ.0) GO TO 1
   IF(ICHECK.EQ.2) GO TO 4
   IF(ICHECK.EQ.4)
     RMAG1=ALOG10(R*MAG1)
     RMAG2=ALOG10(R*MAG2)
     GO TO 5
4 READ(5,105) RMAG1,RMAG2
5 SET1=DATA(IISP1)
  SET2=DATA(IISP2)
  COEF=(RMAG2-RMAG1)/(SET2-SET1)
  ICP=OP
  DO 2 N=1,ICP
    SNUM=(DATA(N)-SET1)*COEF+RMAG1
    RN=N
    FQ=RN*FQ1+F8L
106 WRITE(2,106) SNUM
2 FORMAT(E20.10)
   CONTINUE
   ENO

```

References

1. Rubin, S., and Biehl, F. A., "Mechanical Impedance Approach to Engine Vibration Transmission into an Aircraft Fuselage," SAE Report, No. 670873, 1968.
2. Noiseux, D. U., and Meyer, E. B., "Application of Impedance Theory and Measurements to Structural Vibration," Technical Report AFFDL-TR-67-182, August 1968.
3. O'Hara, G. J., "Mechanical Impedance and Mobility Concepts," The Journal of the Acoustical Society of America, Vol. 41, No. 5, 1967, 1180-1184.
4. Schloss, F., "Recent Advances in the Measurement of Structural Impedance," SAE Report, No. 426B, 1961.
5. Wilcoxon Research, Bulletins One Through Ten, 1. "Weight Limitations of Accelerometers for High Frequency Vibration Measurements," 2. "Choosing an Impedance Head," 3. "Strain Sensitivity of Accelerometers," 4. "Inherent Limitations of Measurable Impedances," 5. "Charge Amplifiers, Disadvantages and Misconceptions," 6. "A Method of Generating Pure Lineal Motion Over an Extended Frequency Range Using Conventional Vibration Generators," 7. "Pressure Sensitivity of Accelerometers and Cables," 8. "New Small Vibration Generators for Mechanical Impedance Applications," 9. "The Effects of Electrical Termination of a Piezoelectric Transducer on its Frequency Response," 10. "Accelerometers for Model Testing."
6. Control and Communication Division, Instruction Manual, Data Acquisition System MIT Laboratory, Radiation Incorporated.
7. Spectral Dynamics Corporation of San Diego, Instruction Manual SD 1002B-33 Automatic Mechanical Impedance System, August 1968.
8. Snowdon, J. C., "Mechanical Impedance of Free-Free Beams," The Journal of the Acoustical Society of America, Vol. 37, No. 2, February 1965, 240-249.
9. Den Hartog, J. P., Mechanical Vibrations, 4th ed., McGraw-Hill Book Company, Inc., N. Y., 1956, 432.

10. Logcher, R. D.; Flachsbart, B. B.; Hall, E. J.; Power, C. M.; Wells, R. A., Jr.; Ferrante, A. J.; "Volume 1 Frame Analysis," ICES STRUDL-II The Structural Design Language Engineering User's Manual, Research Report R68-91, Structures Division and Civil Engineering Systems Laboratory, Department of Civil Engineering, Massachusetts Institute of Technology, Cambridge, Massachusetts, November 1968.
11. Logcher, R. D.; Connor, J. J., Jr.; Ferrante, A. J.; "Volume 2 Additional Design and Analysis Facilities," ICES STRUDL-II The Structural Design Language Engineering User's Manual, Research Report R68-92, Structures Division and Civil Engineering Systems Laboratory, Department of Civil Engineering, Massachusetts Institute of Technology, Cambridge, Massachusetts, June 1969.
12. Przemieniecki, J. S., Theory of Matrix Structural Analysis, McGraw-Hill Book Company, Inc., N. Y., 1968, 434.

| DOCUMENT CONTROL DATA - R&D | | |
|--|--|--|
| <i>(Security classification of title, body of abstract and indexing annotation must be entered when the overall report is classified)</i> | | |
| 1. ORIGINATING ACTIVITY (Corporate author) Lincoln Laboratory, M.I.T. | | 2a. REPORT SECURITY CLASSIFICATION Unclassified |
| | | 2b. GROUP None |
| 3. REPORT TITLE The Analysis of Two Simple Composite Structures Using Mechanical Admittance Methods | | |
| 4. DESCRIPTIVE NOTES (Type of report and inclusive dates) Technical Note | | |
| 5. AUTHOR(S) (Last name, first name, initial) Bagley, Ronald L. | | |
| 6. REPORT DATE 7 September 1971 | 7a. TOTAL NO. OF PAGES 120 | 7b. NO. OF REFS 12 |
| 8a. CONTRACT OR GRANT NO. F19628-70-C-0230 | 9a. ORIGINATOR'S REPORT NUMBER(S) Technical Note 1971-40 | |
| b. PROJECT NO. 649L | 9b. OTHER REPORT NO(S) (Any other numbers that may be assigned this report) ESD-TR-71-262 | |
| c. | | |
| d. | | |
| 10. AVAILABILITY/LIMITATION NOTICES Approved for public release; distribution unlimited. | | |
| 11. SUPPLEMENTARY NOTES None | 12. SPONSORING MILITARY ACTIVITY Air Force Systems Command, USAF | |
| 13. ABSTRACT <p>Mechanical admittance methods are applied to two simple composite structures. The mechanical admittances of the composite structures are predicted using the mechanical admittances measured on their constituent substructures. The effects of the suspension system on the measured admittances are estimated. Attention is devoted to the technique of analytically assembling substructures into a composite structure.</p> <p>Resonant frequencies and mode shapes of the composite structures are estimated from the predicted admittances. The effects of modal participation and damping on the estimated mode shapes and resonant frequencies are discussed.</p> | | |
| 14. KEY WORDS mechanical admittance mechanical impedance mode shape acoustical transmission resonant frequencies | | |